Supporting Information

Extremely stable system of 1-haloselanyl-anthraquinones: Experimental and theoretical investigations

Naoki Ogawa,[a] Nobuhiro Suzuki,[a] Yoshifumi Katsura,[a] Mao Minoura,[b] Waro Nakanishi[a] and Satoko Hayashi* [a]

[a] *Faculty of Systems Engineering, Wakayama University, 930 Sakaedani, Wakayama 640-8510, Japan. E-mail: hayashi3@sys.wakayama-u.ac.jp*
[b] *Department of Chemistry, College of Science, Rikkyo University, Toshima-ku, Tokyo, 171-8501, Japan*

Table of Contents

Table S1. The r_{BP} and R_{SL} values evaluated with MP2/BSS-A for the optimized structures of **1**–**7** evaluated with MP2/BSS-A, and **8** evaluated with MP2/BSS-B, together with the Δr_{BP} values.

Compound	r_{BP}[a] (Å)	R_{SL}[b] (Å)	Δr_{BP}[c] (Å)
Se-∗-O_1			
1	2.3817	2.3803	0.0014
2	2.3102	2.3089	0.0012
3	2.2795	2.2784	0.0012
4	2.1873	2.1863	0.0010
5	2.6372	2.6359	0.0013
6	2.6293	2.6275	0.0018
8	2.6029	2.6013	0.0016
Se-∗-X			
1	2.5581	2.5574	0.0007
2	2.3721	2.3717	0.0005
3	2.2279	2.2275	0.0004
4	1.8103	1.8101	0.0002
5	1.4543	1.4623	-0.0079
6	1.9398	1.9393	0.0005
8	2.3405	2.3391	0.0015
Se-∗-Br			
7	2.9190	2.9168	0.0022

[a] The lengths of BPs. [b] Straight-line distances. [c] $\Delta r_{BP} = r_{BP} - R_{SL}$.

Table S2. QTAIM functions and QTAIM-DFA parameters for **II** and **IV**, evaluated with MP2/BSS-A.[a,b]

species	$\rho_b(\boldsymbol{r}_c)$ (au)	$c\nabla^2\rho_b(\boldsymbol{r}_c)$ [c] (au)	$H_b(\boldsymbol{r}_c)$ (au)	R[d] (au)	θ[e] (°)	θ_p[f] (°)	κ_p[g] (au^{-1})	C_{ii} (Å $mdyn^{-1}$)	predicted nature
Se-∗-O_1									
II (I)	0.0382	0.0142	-0.0017	0.0143	96.9	141.2	101.0	3.59	*r*-CS/*t*-HB_{wc}
II (Br)	0.0459	0.0157	-0.0049	0.0164	107.2	158.0	56.9	3.44	*r*-CS/CT-MC
II (Cl)	0.0496	0.0163	-0.0068	0.0176	112.6	163.4	39.8	3.29	*r*-CS/CT-MC
II (F)	0.0647	0.0177	-0.0169	0.0244	133.7	173.5	5.7	2.41	*r*-CS/CT-MC
II (H)	0.0220	0.0096	0.0017	0.0098	80.0	95.6	84.9	3.52	*p*-CS/*t*-HB_{nc}
II (Me)	0.0220	0.0096	0.0016	0.0098	80.4	95.6	83.0	3.48	*p*-CS/*t*-HB_{nc}
IV (I)	0.0263	0.0107	0.0008	0.0107	85.5	110.3	121.1	5.36	*p*-CS/*t*-HB_{nc}
IV (Br)	0.0311	0.0122	-0.0001	0.0122	90.3	124.3	125.6	4.36	*r*-CS/*t*-HB_{wc}
IV (Cl)	0.0330	0.0128	-0.0005	0.0128	92.4	130.2	119.5	3.99	*r*-CS/*t*-HB_{wc}
IV (F)	0.0404	0.0146	-0.0032	0.0150	102.5	149.2	73.2	2.79	*r*-CS/*t*-HB_{wc}
IV (H)	0.0158	0.0070	0.0016	0.0072	76.9	86.2	58.2	7.37	*p*-CS/vdW
IV (Me)	0.0153	0.0067	0.0016	0.0069	77.0	85.6	53.1	7.74	*p*-CS/vdW
Se-∗-X									
II (I)	0.0859	-0.0014	-0.0344	0.0344	182.4	192.0	0.8	0.64	SS/Cov-w
II (Br)	0.0970	0.0003	-0.0412	0.0412	179.6	191.1	0.7	0.60	*r*-CS/CT-TBP + X_3^-
II (Cl)	0.1092	0.0006	-0.0551	0.0551	179.4	186.3	3.5	0.56	*r*-CS/CT-TBP + X_3^-
II (F)	0.1408	0.0402	-0.0856	0.0946	154.8	144.1	4.4	0.36	*r*-CS/*t*-HB_{wc}
II (H)	0.1810	-0.0320	-0.1506	0.1540	192.0	178.1	4.2	0.28	SS/Cov-s
II (Me)	0.1522	-0.0198	-0.0982	0.1002	191.4	189.1	4.0	0.37	SS/Cov-w
IV (I)	0.0887	-0.0023	-0.0369	0.0370	183.5	191.7	0.5	0.55	SS/Cov-w
IV (Br)	0.1012	-0.0010	-0.0451	0.0451	181.3	190.9	0.3	0.51	SS/Cov-w
IV (Cl)	0.1145	-0.0006	-0.0606	0.0606	180.6	184.6	4.0	0.46	SS/Cov-w
IV (F)	0.1470	0.0448	-0.0921	0.1024	154.1	142.0	3.1	0.30	*r*-CS/*t*-HB_{wc}
IV (H)	0.1817	-0.0323	-0.1516	0.1550	192.0	178.1	4.2	0.27	SS/Cov-s
IV (Me)	0.1517	-0.0198	-0.0974	0.0994	191.5	189.4	3.9	0.37	SS/Cov-w

[a] See text for BSS-A. [b] Data are given at BCP, which is shown by A-∗-B, where one side interaction is shown if two are identical due to the symmetry. [c] $c\nabla^2\rho_b(\boldsymbol{r}_c) = H_b(\boldsymbol{r}_c) - V_b(\boldsymbol{r}_c)/2$, where $c = \hbar^2/8m$. [d] $R = (x^2 + y^2)^{1/2}$, where $(x, y) = (H_b(\boldsymbol{r}_c) - V_b(\boldsymbol{r}_c)/2, H_b(\boldsymbol{r}_c))$. [e] $\theta = 90^o - \tan^{-1}(y/x)$, where $(x, y) = (H_b(\boldsymbol{r}_c) - V_b(\boldsymbol{r}_c)/2, H_b(\boldsymbol{r}_c))$. [f] $\theta_p = 90^o - \tan^{-1}(dy/dx)$. [g] $\kappa_p = |d^2y/dx^2| / [1 + (dy/dx)^2]^{3/2}$.

Table S3. The carbonyl stretching frequencies calculated and/or observed for **1**–**8**.

Species/No	ν_{calcd} (C=O)[a]	ν_{calcd} (C=O)[b]	ν_{obsd} (C=O)
1	1632.7; 1690.1	1633.9; 1684.2	1635; 1680
2	1630.3; 1689.4	1631.3; 1683.7	*c*
3	1629.9; 1689.2	1630.9; 1683.5	*c*
4	1629.4; 1687.7	1630.6; 1682.2	*c*
5	1666.9; 1692.3	1664.6; 1685.9	*c*
6	1663.1; 1691.3	1661.6; 1685.0	1667
7	1684.2; 1697.5	1682.4; 1691.4	1681
8	*c*	1656.5; 1685.3	*c*

[a] Under MP2/BSS-A. [b] Under MP2/BSS-B. [c] Not obtained.

The IR spectra could be measured only for **1**, among **1**–**5**. **1** was decomposed during the preparation of the disk for the measure with KCl. Therefore, a PTFE IR card was used for the measurement. Measurements of **3**–**5** were not tried, since we do not have the samples, so was **8**. Two strong and two weak signals appeared in the C=O stretching region in **6**. Two of them seem to be ν_s (C=O) and ν_{as} (C=O), whereas other two could arise from the interactions between ν (C=O) and the vibrations from the aryl moiety. The two strong ν (C=O) values, very close the predicted values, are selected, as shown in Table 6 of the text. Only one ν_{obsd} (C=O) signal is obtained for **7**, which can be assigned to ν_{as} (C=O).

The ν_{calcd} (C=O) values obtained under MP2/BSS-B are very close to the corresponding values, respectively, obtained under MP2/BSS-A. The ν_{obsd} (C=O) values are very close to the corresponding ν_{calcd} (C=O) values, respectively, obtained under MP2/BSS-B, although the adjustment of the calculated method is not considered.

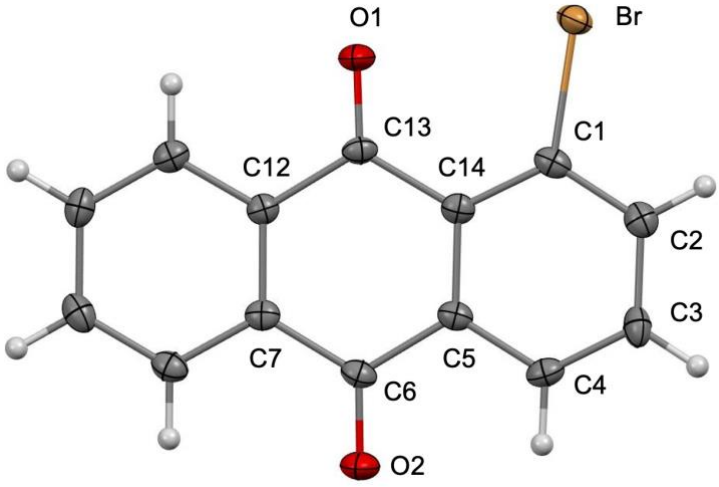

Fig. S1 Observed structures of **7**.

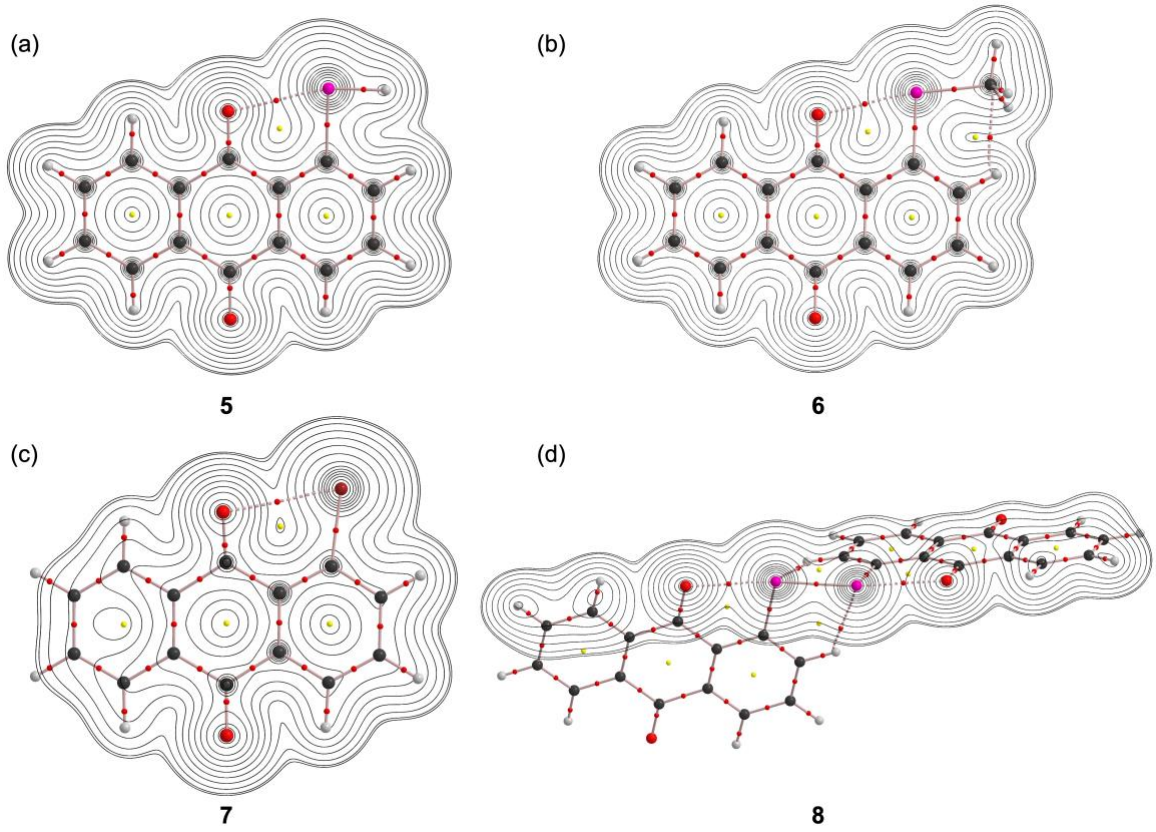

Fig. S2 Molecular graphs with contour plots for **5**–**7** calculated with MP2/BSS-A and **8** with MP2/BSS-B (shown by (a)–(d), respectively). The BCPs are denoted by red dots, RCPs are indicated by yellow dots and BPs are indicated by pink lines. The carbon, hydrogen, oxygen, selenium and bromine atoms are shown in black, grey, red, magenta and brown, respectively. Contour plots are drawn on the planes containing the O---Se–X interaction for each.

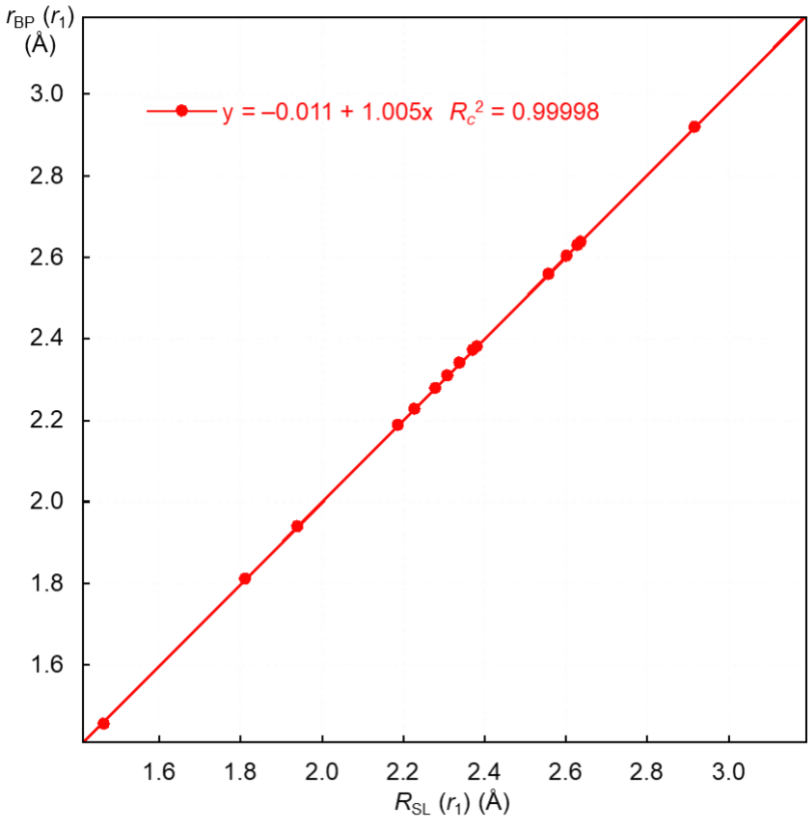

Fig. S3 Plot of $r_{BP}(r_1)$ versus $R_{SL}(r_1)$ for the optimized structures of **1**–**7** evaluated with MP2/BSS-A, and **8** evaluated with MP2/BSS-B. See Chart 1 and Fig. 2 in the text.

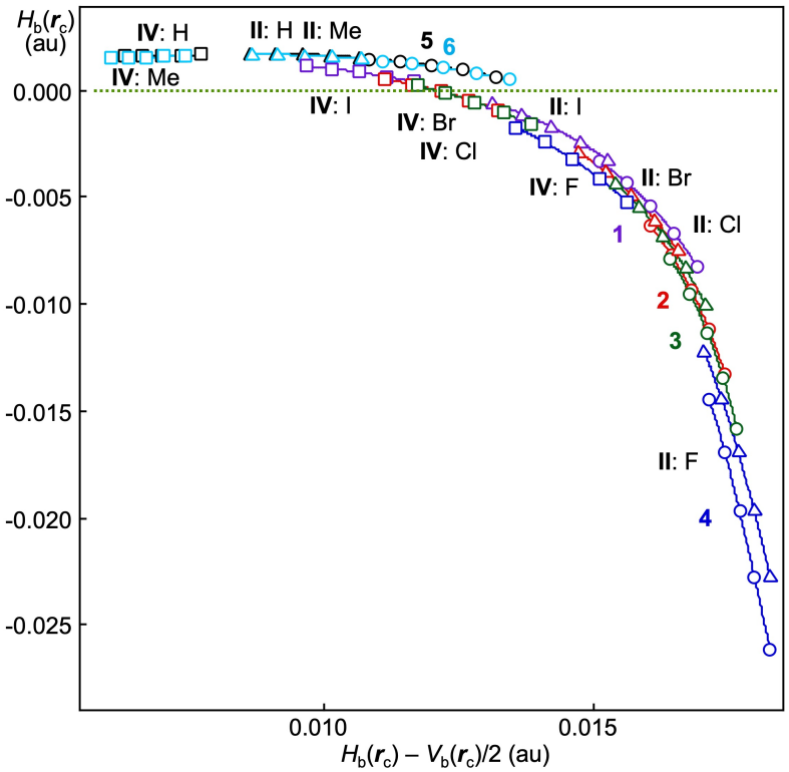

Fig. S4 Plots of $H_b(r_c)$ versus $H_b(r_c) - V_b(r_c)/2$ for O-∗-Se from the fully optimized structures and the perturbed structures generated with CIV for **1–6**, **II** and **IV**.

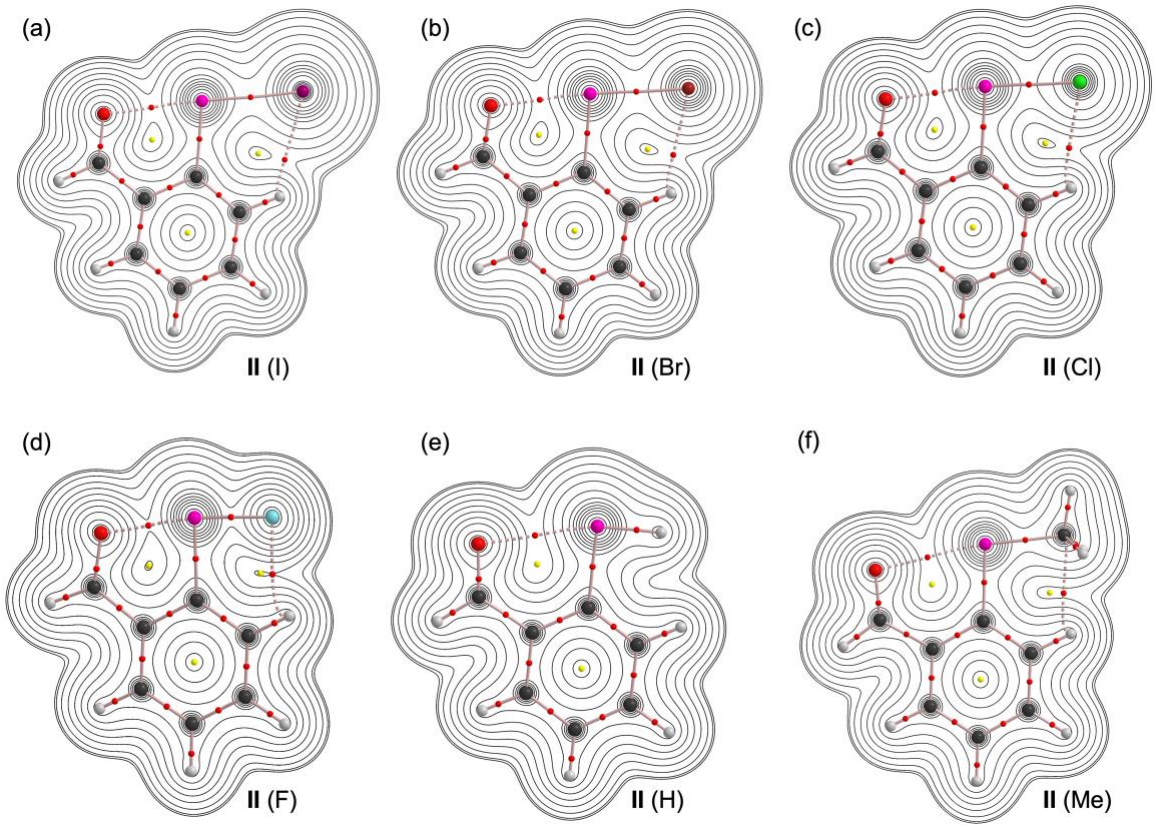

Fig. S5 Molecular graphs with contour plots for **II** (I)–**II** (Me) calculated with MP2/BSS-A (shown by (a)–(f), respectively). The BCPs are denoted by red dots, RCPs are indicated by yellow dots and BPs are indicated by pink lines. The carbon, hydrogen, oxygen, selenium, iodine, bromine, chlorine and fluorine atoms are shown in black, grey, red, magenta, purple, brown, light green and light blue. respectively. Contour plots are drawn on the planes containing the O---Se–X interaction for each.

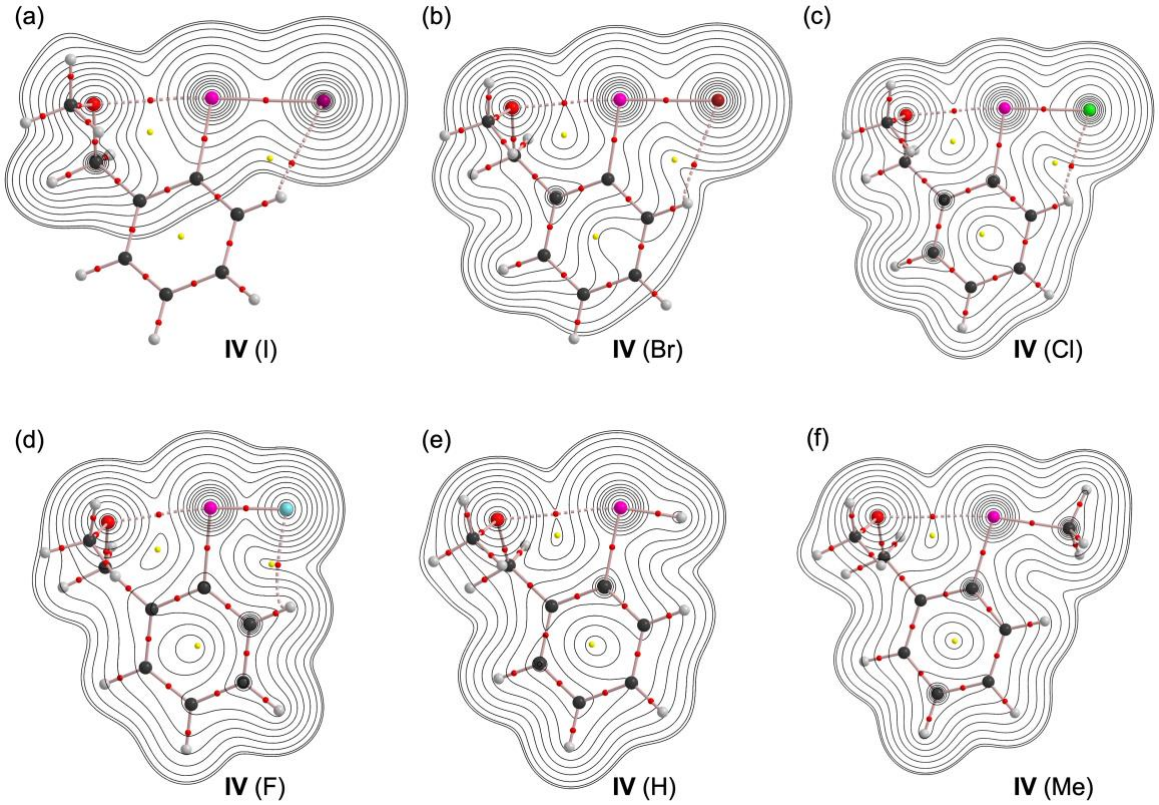

Fig. S6 Molecular graphs with contour plots for **IV** (I)–**IV** (Me) calculated with MP2/BSS-A (shown by (a)–(f), respectively). The BCPs are denoted by red dots, RCPs are indicated by yellow dots and BPs are indicated by pink lines. The carbon, hydrogen, oxygen, selenium, iodine, bromine, chlorine and fluorine atoms are shown in black, grey, red, magenta, purple, brown, light green and light blue. respectively. Contour plots are drawn on the planes containing the O---Se–X interaction for each.

(a)

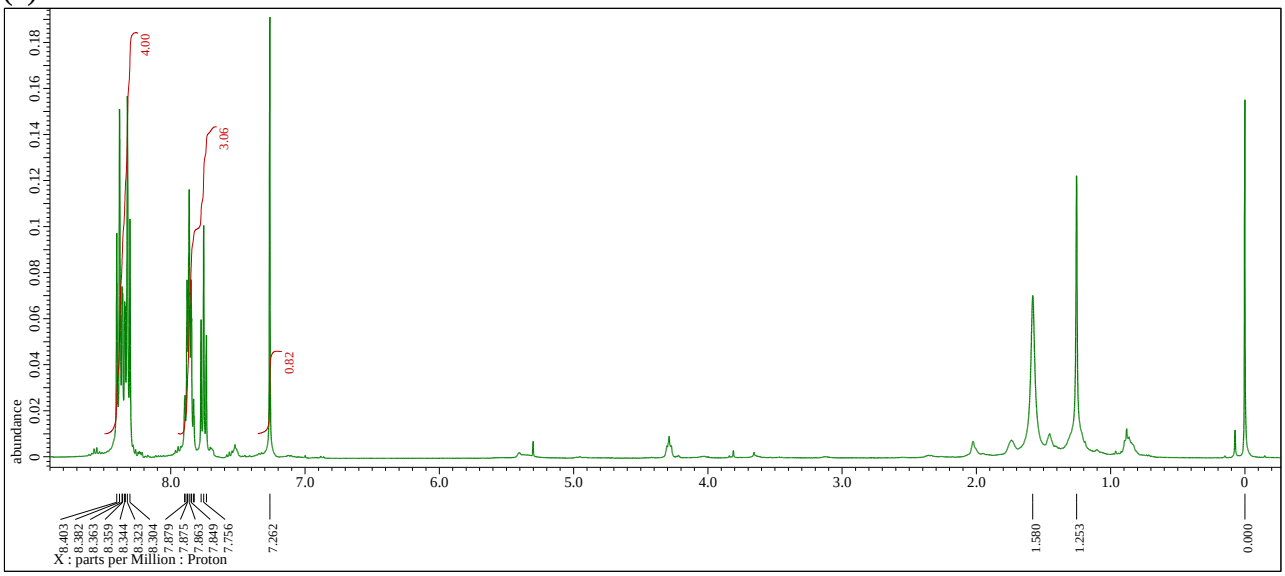

(b)

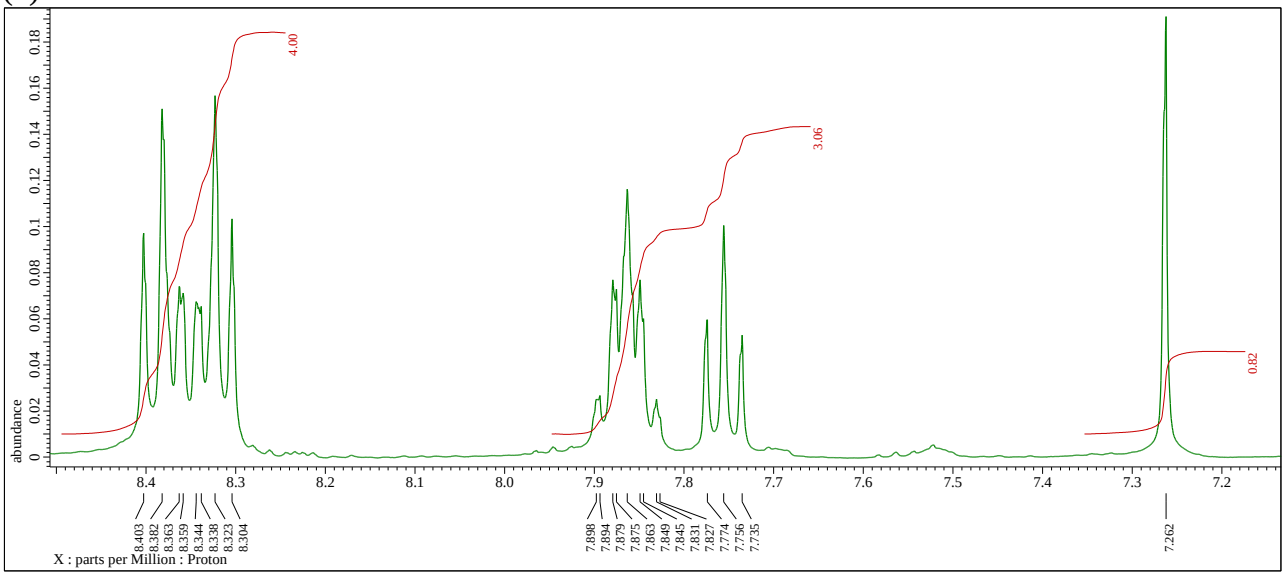

Fig. S7 ^{1}H NMR spectrum of **1**.

(a)

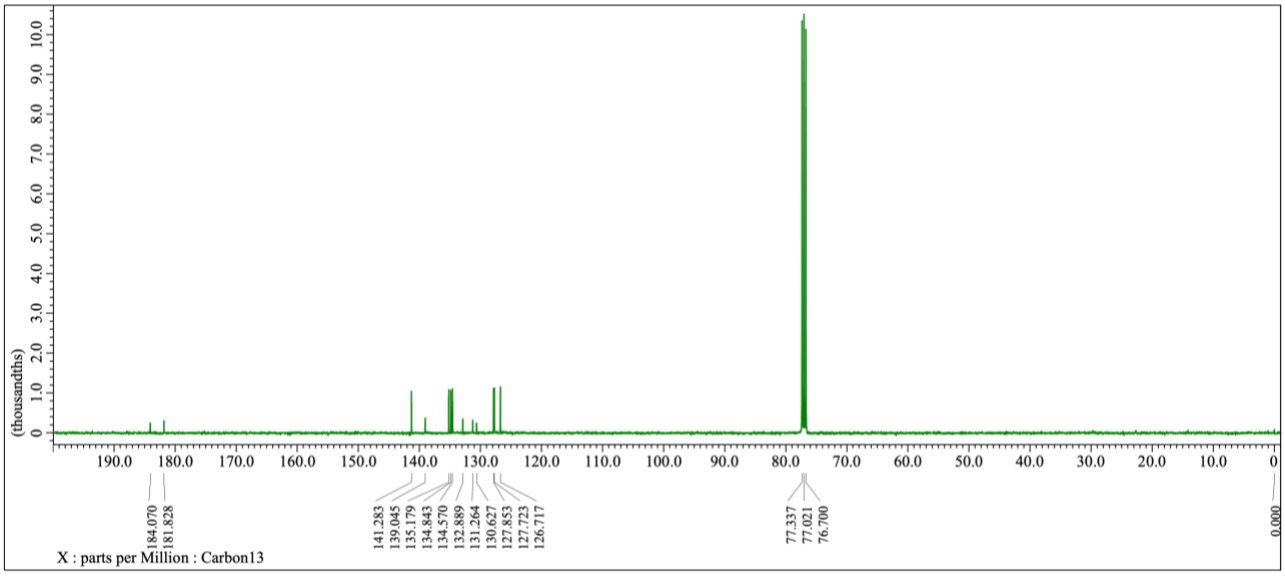

(b)

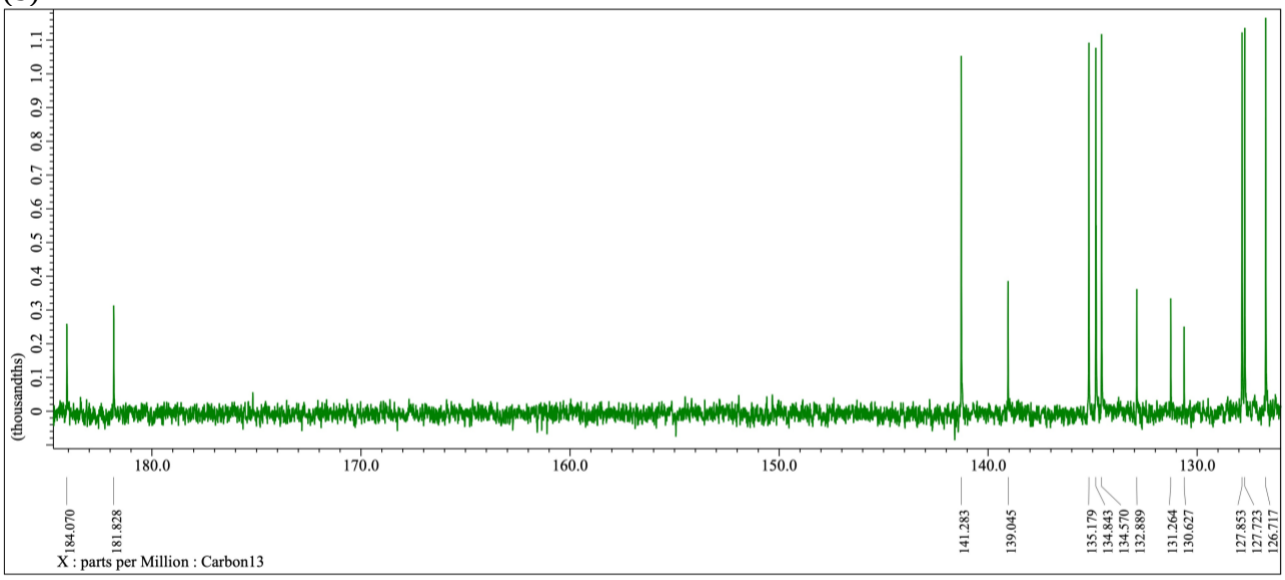

Fig. S8 ^{13}C NMR spectrum of **1**.

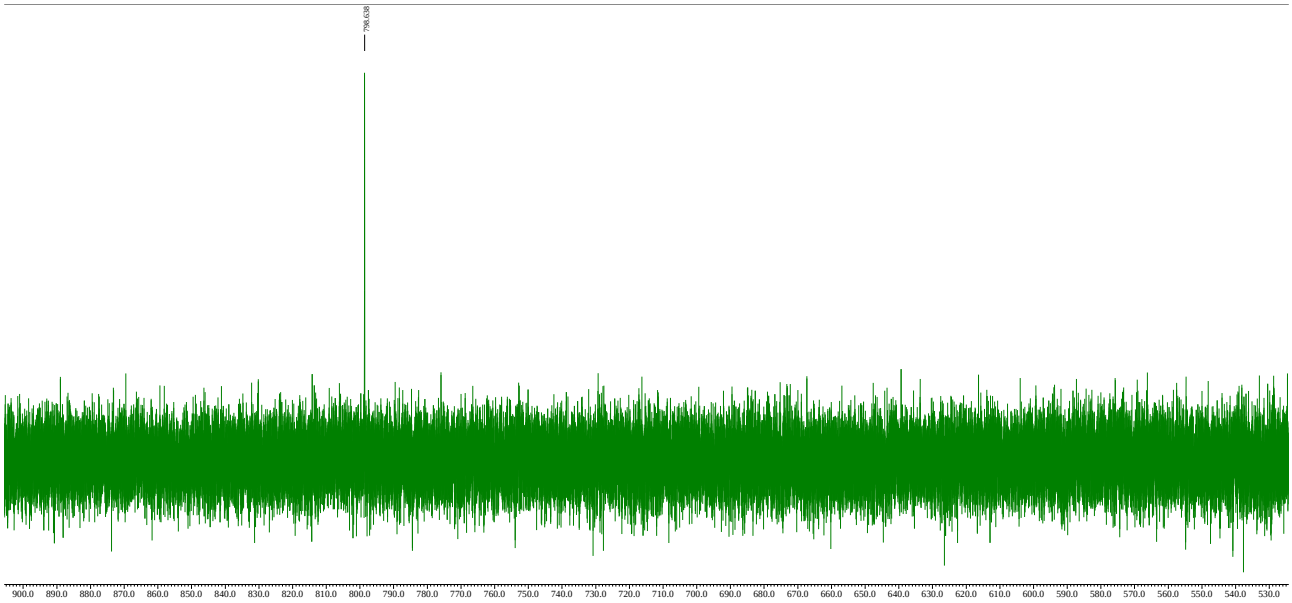

Fig. S9 ^{77}Se NMR spectrum of **1**.

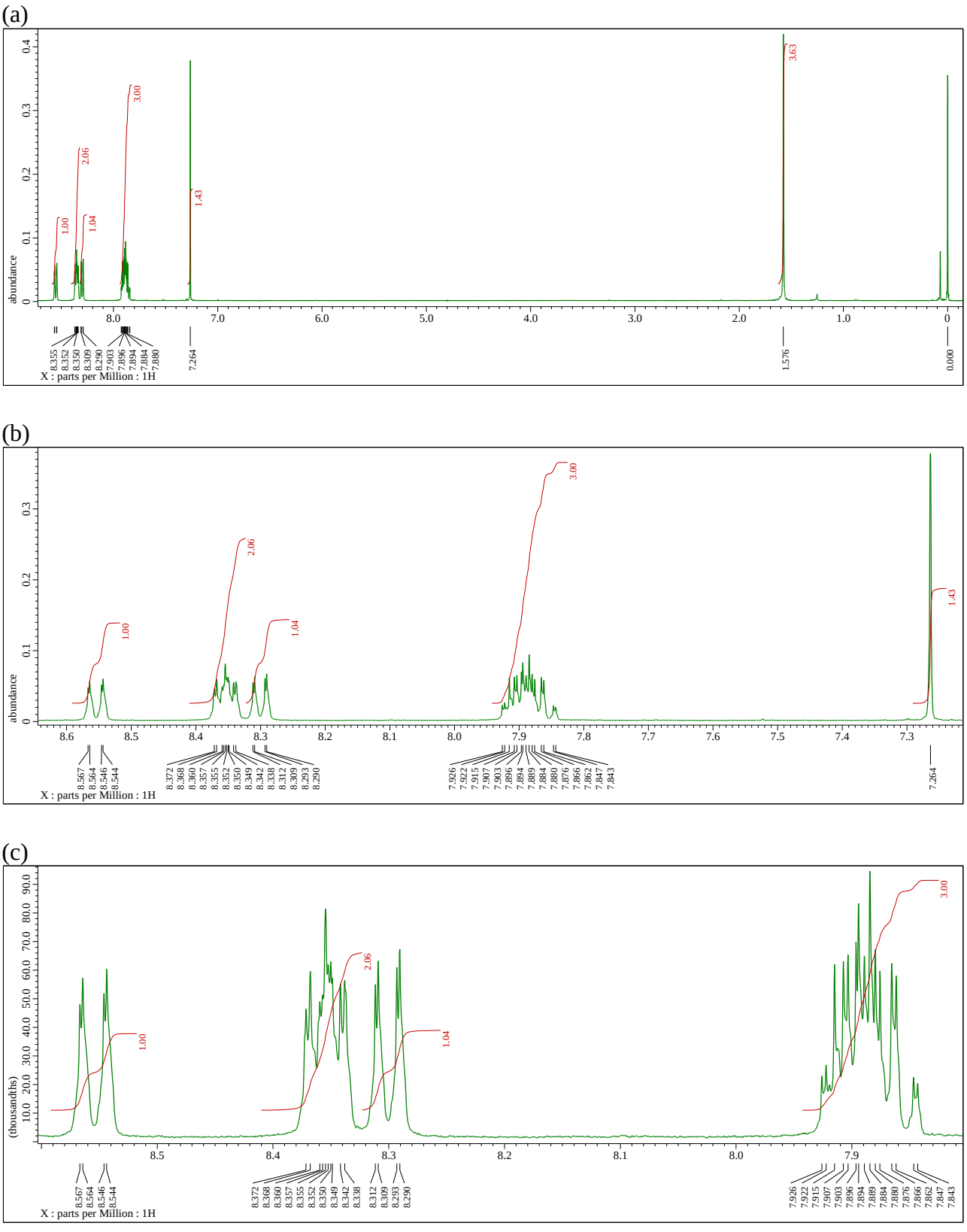

Fig. S10 ^{1}H NMR spectrum of **2**.

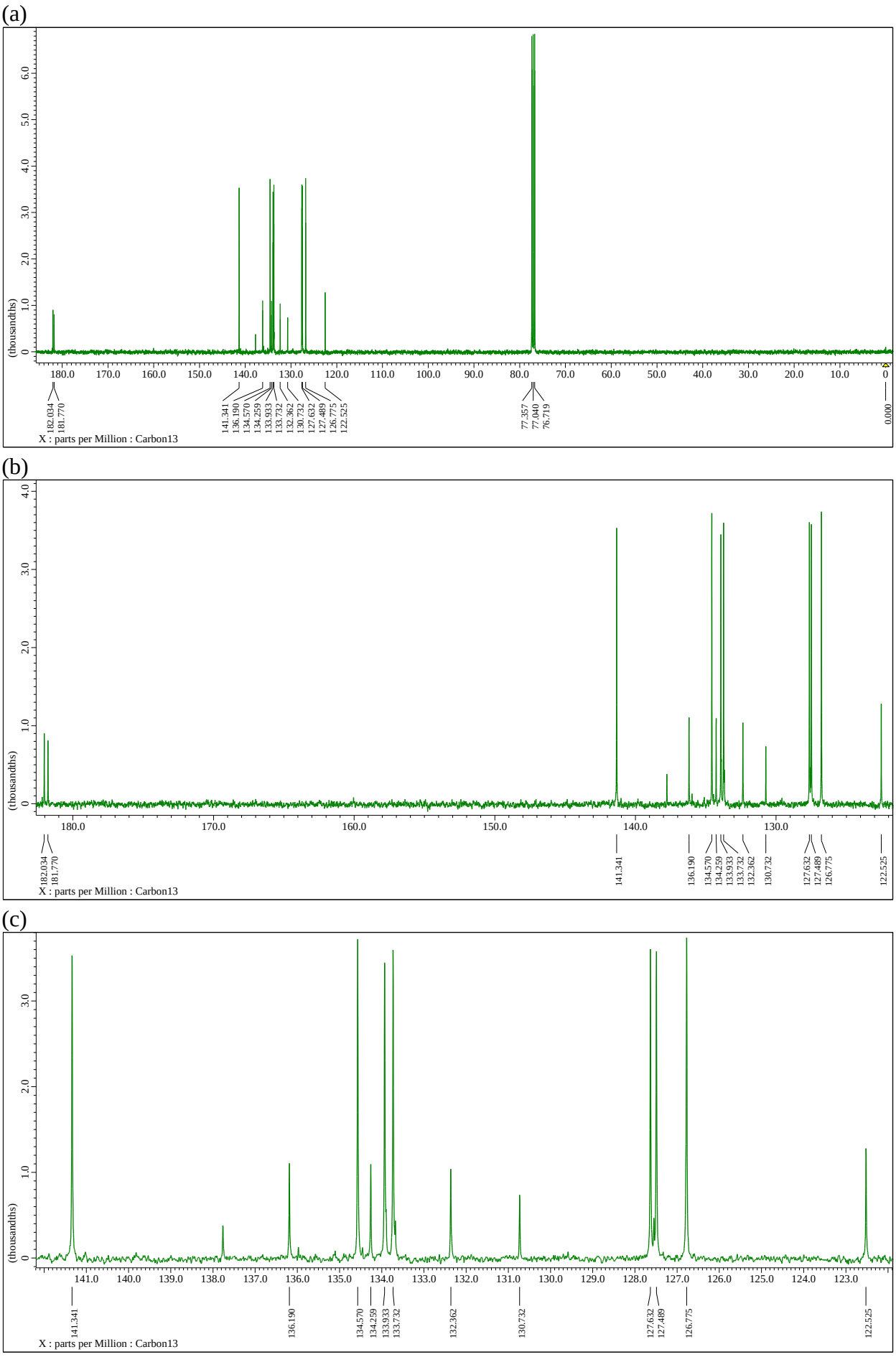

Fig. S11 ^{13}C NMR spectrum of **2**.

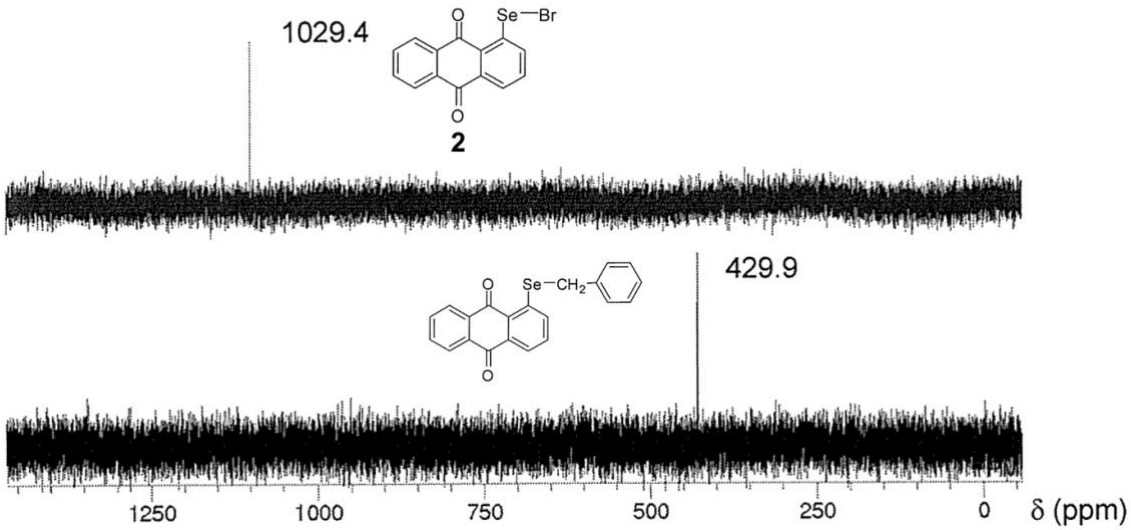

Fig. S12 ^{77}Se NMR spectrum of **2**.

(a)

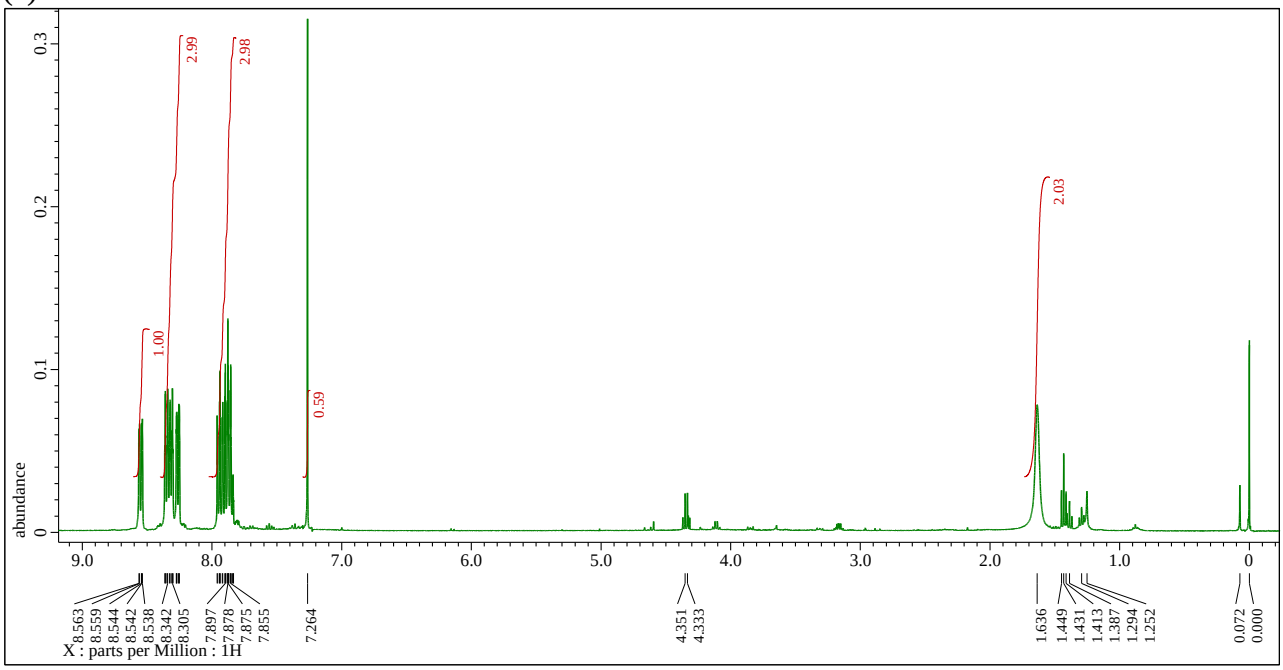

(b)

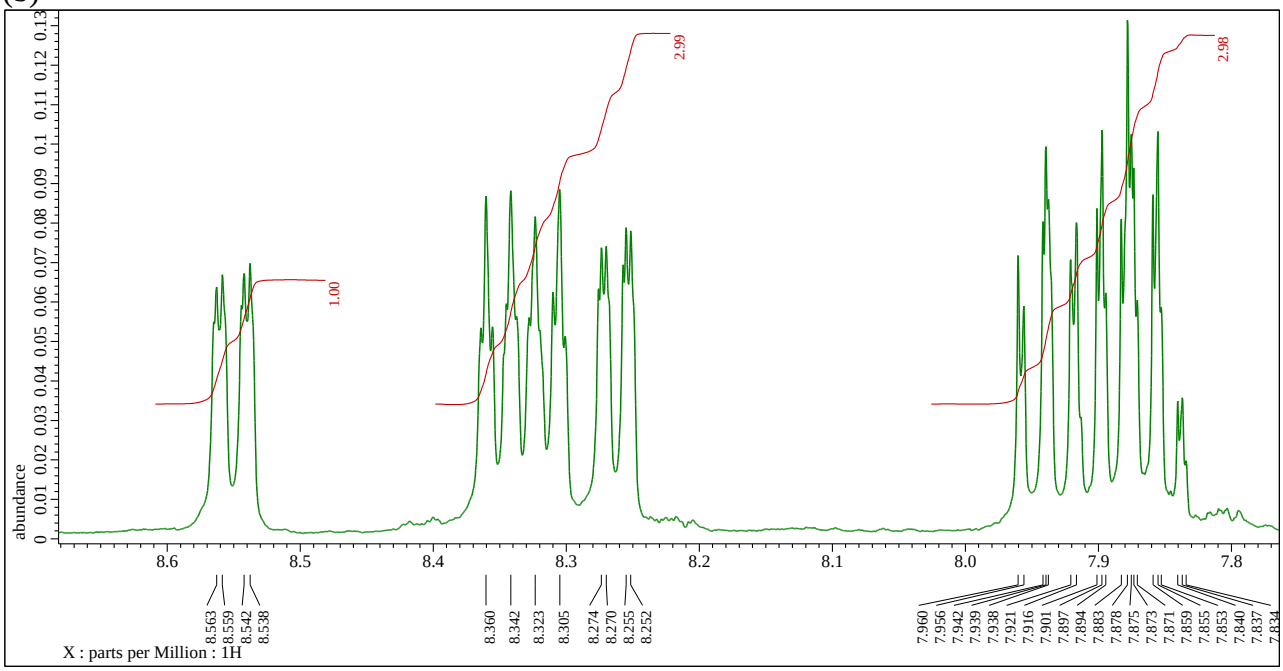

Fig. S13 ^{1}H NMR spectrum of **3**.

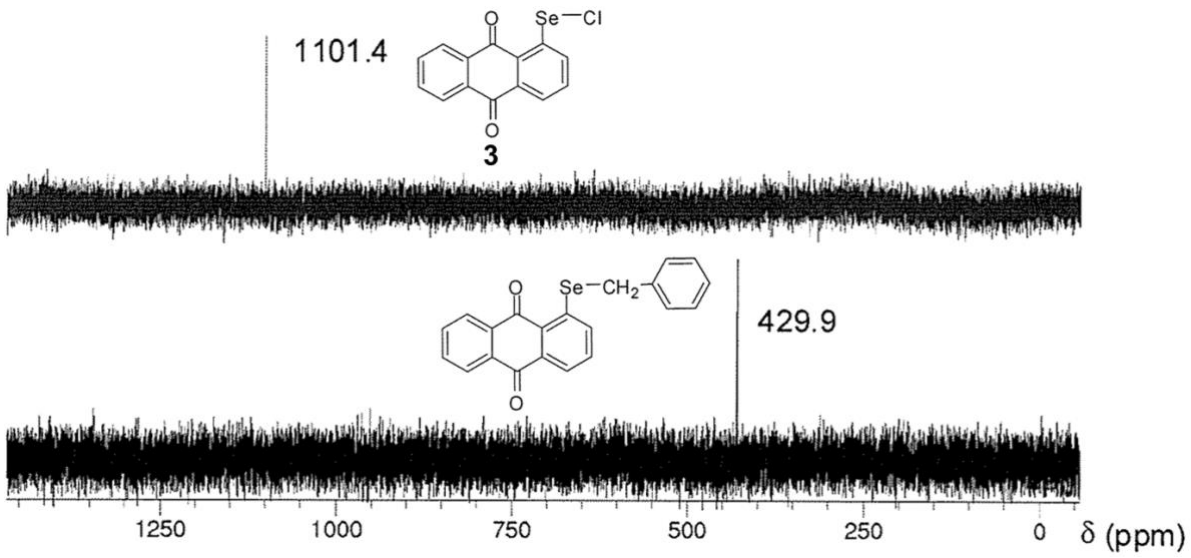

Fig. S14 ^{77}Se NMR spectrum of **3**.

(a)

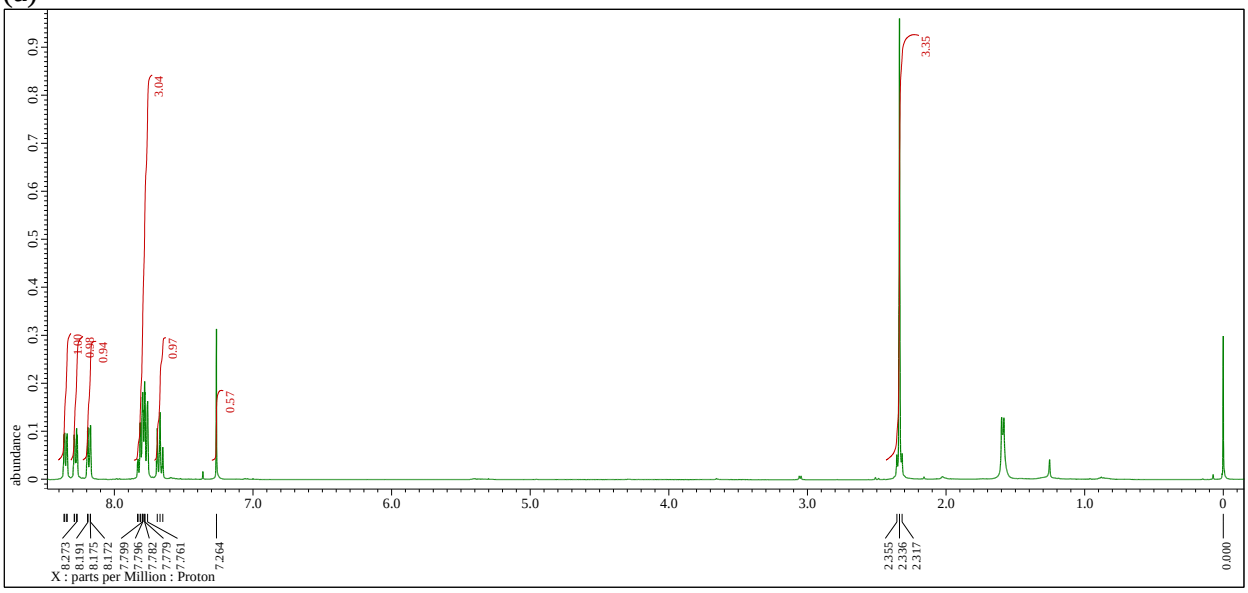

(b)

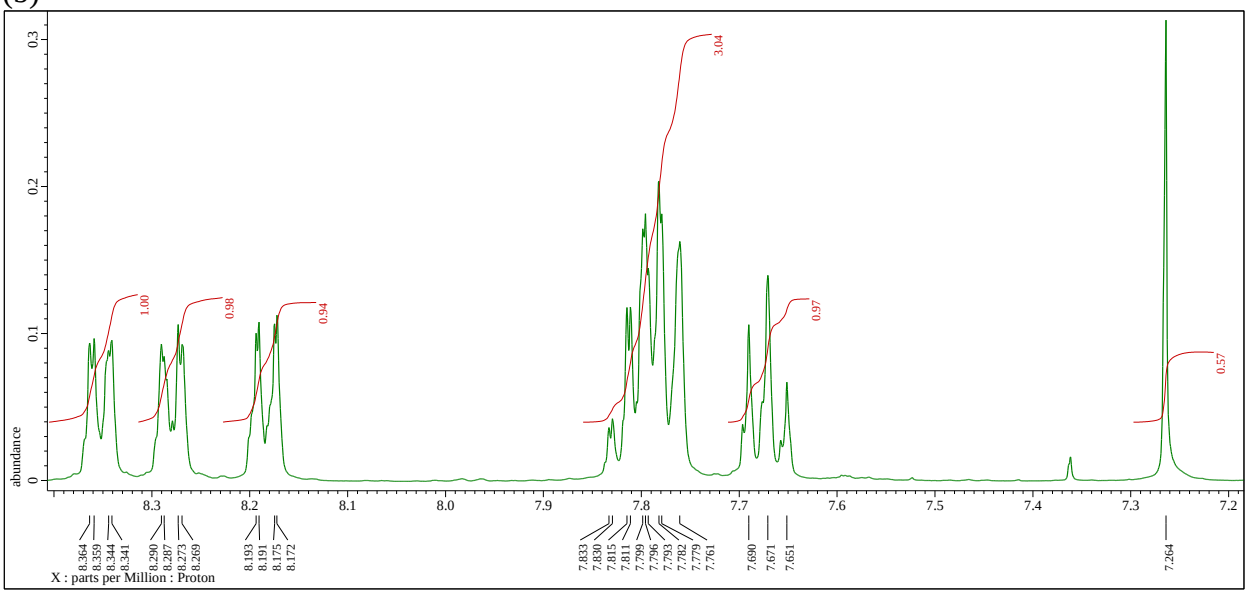

Fig. S15 ^{1}H NMR spectrum of **6**.

(a)

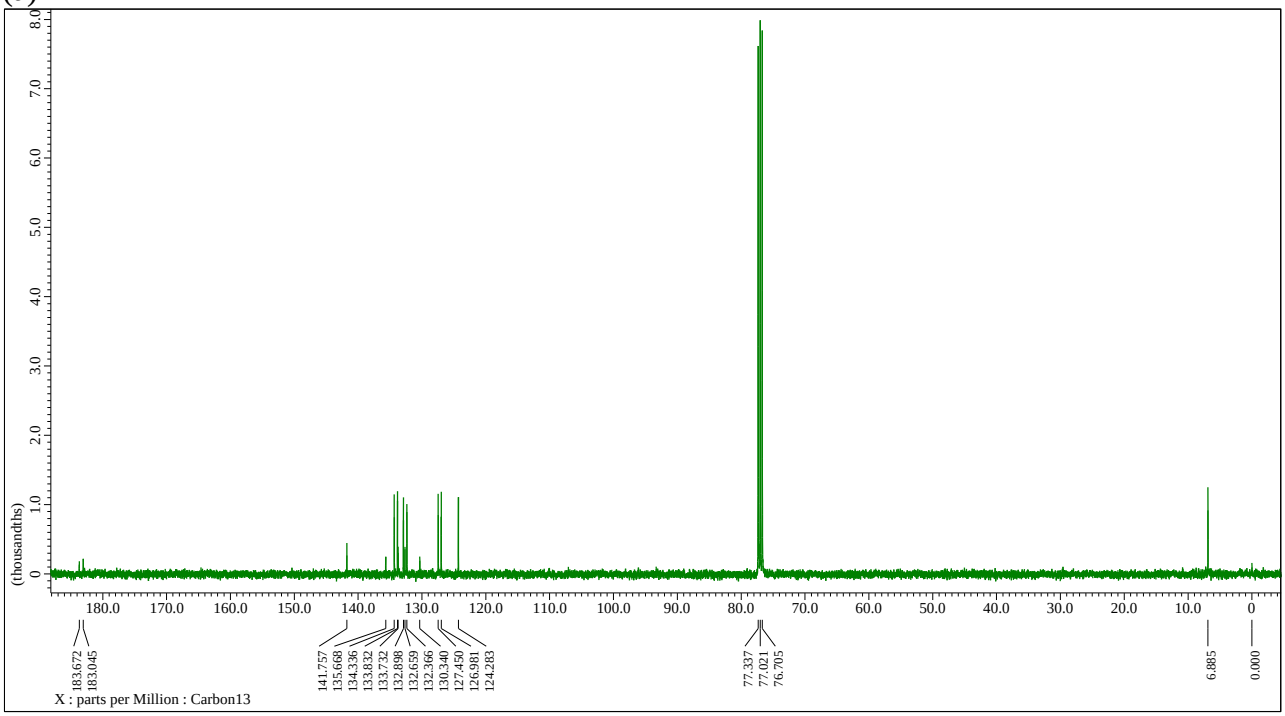
(thousandths)
8.0
7.0
6.0
5.0
4.0
3.0
2.0
1.0
0
180.0
170.0
160.0
150.0
140.0
130.0
120.0
110.0
100.0
90.0
80.0
70.0
60.0
50.0
40.0
30.0
20.0
10.0
0
183.672
183.045
141.757
135.668
134.336
133.832
133.732
132.898
132.659
132.366
130.340
127.450
126.981
124.283
77.337
77.021
76.705
6.885
0.000
X : parts per Million : Carbon13

(b)

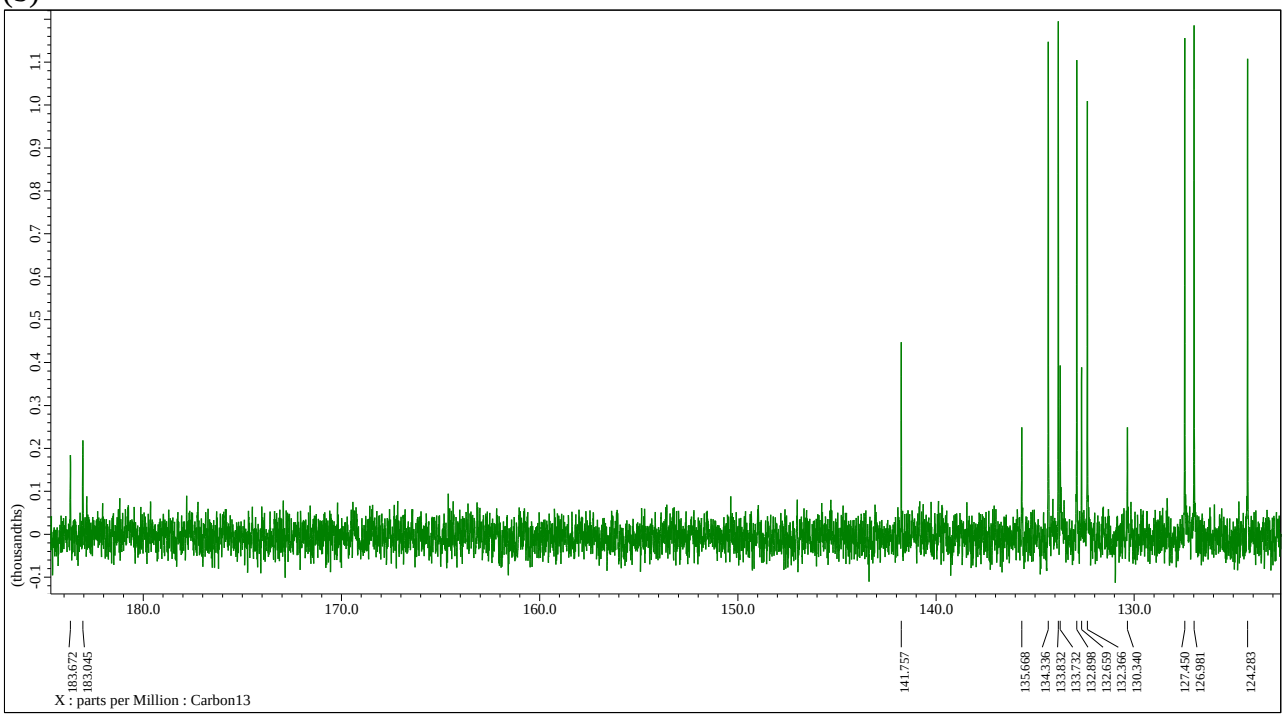
(thousandths)
1.1
1.0
0.9
0.8
0.7
0.6
0.5
0.4
0.3
0.2
0.1
0
-0.1
180.0
170.0
160.0
150.0
140.0
130.0
183.672
183.045
141.757
135.668
134.336
133.832
133.732
132.898
132.659
132.366
130.340
127.450
126.981
124.283
X : parts per Million : Carbon13

(c)

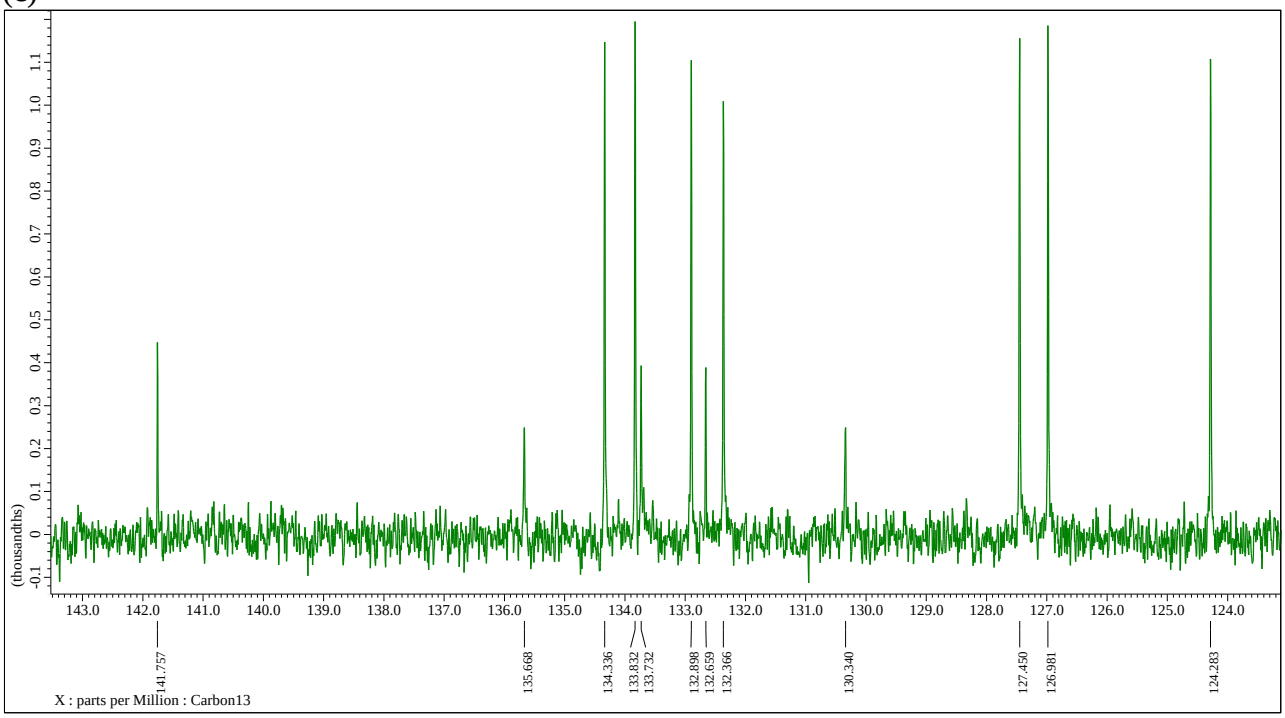

Fig. S16 ^{13}C NMR spectrum of **6**.

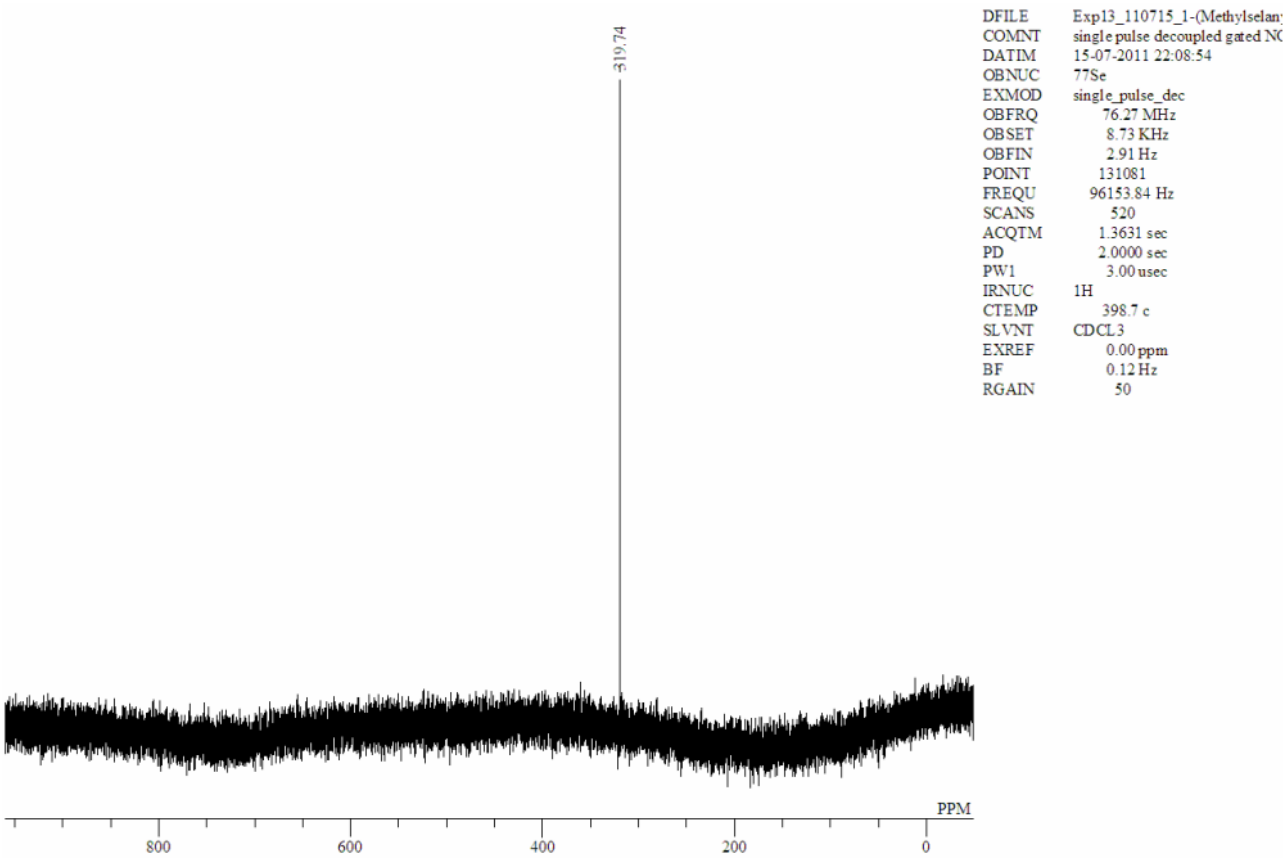

Fig. S17 ^{77}Se NMR spectrum of **6**.

(a)

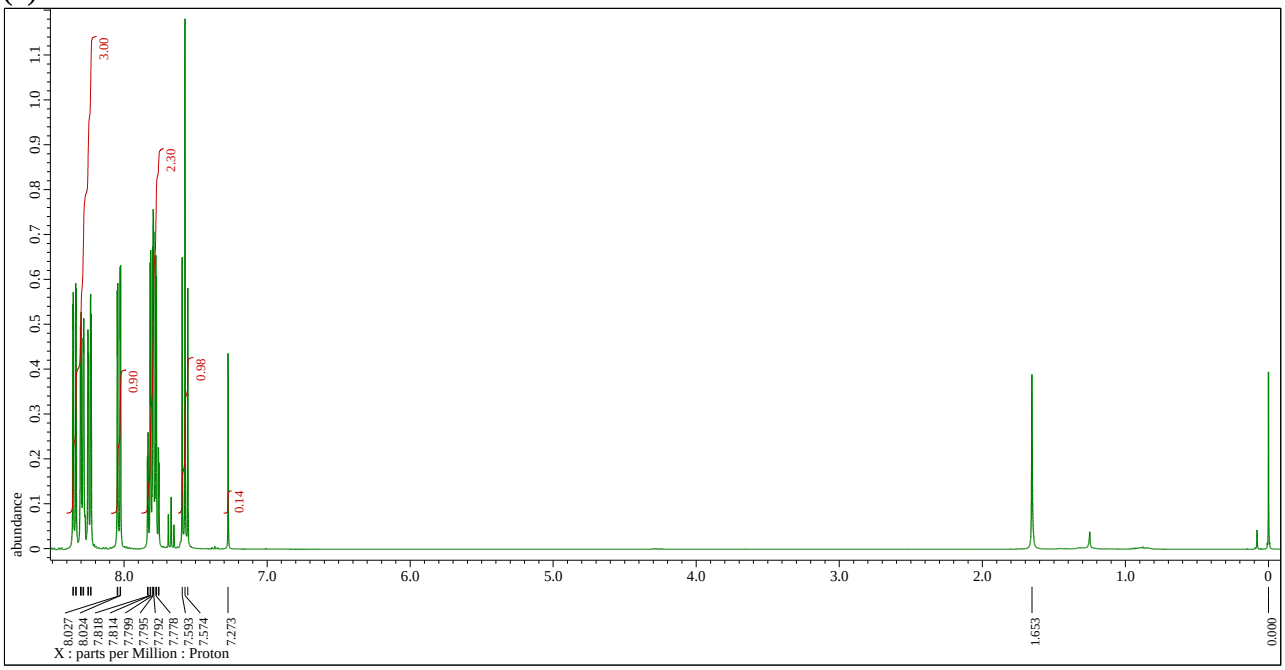

(b)

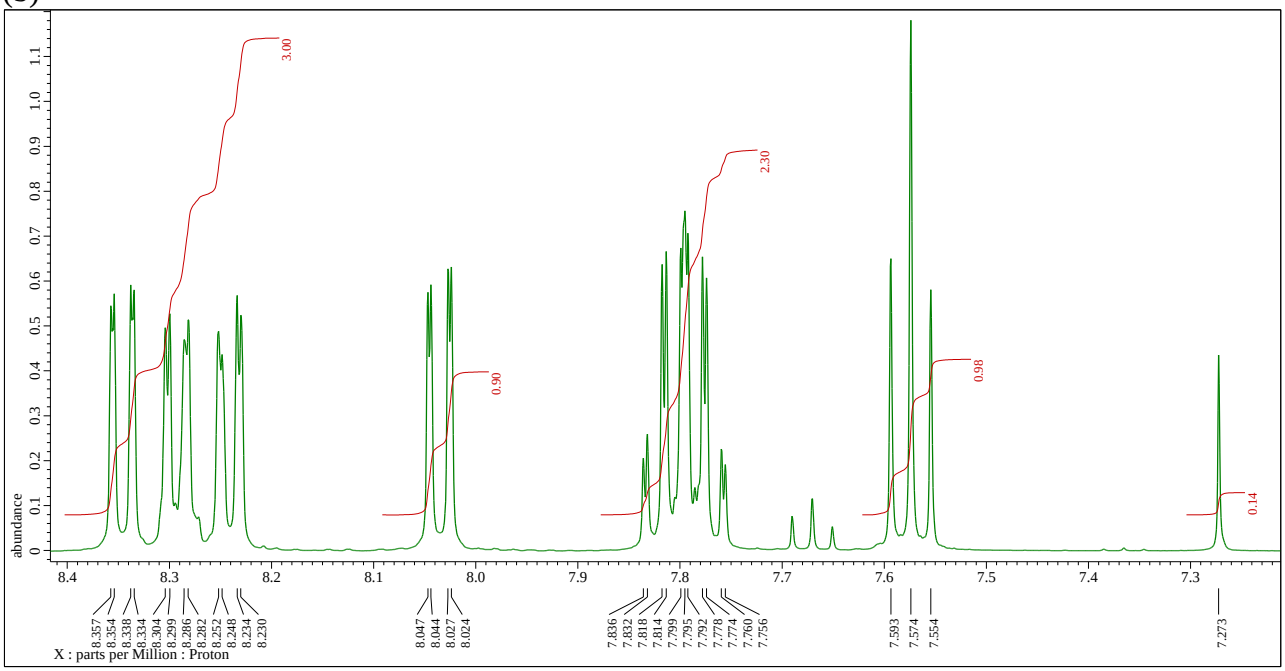

Fig. S18 ^{1}H NMR spectrum of **7**.

(a)

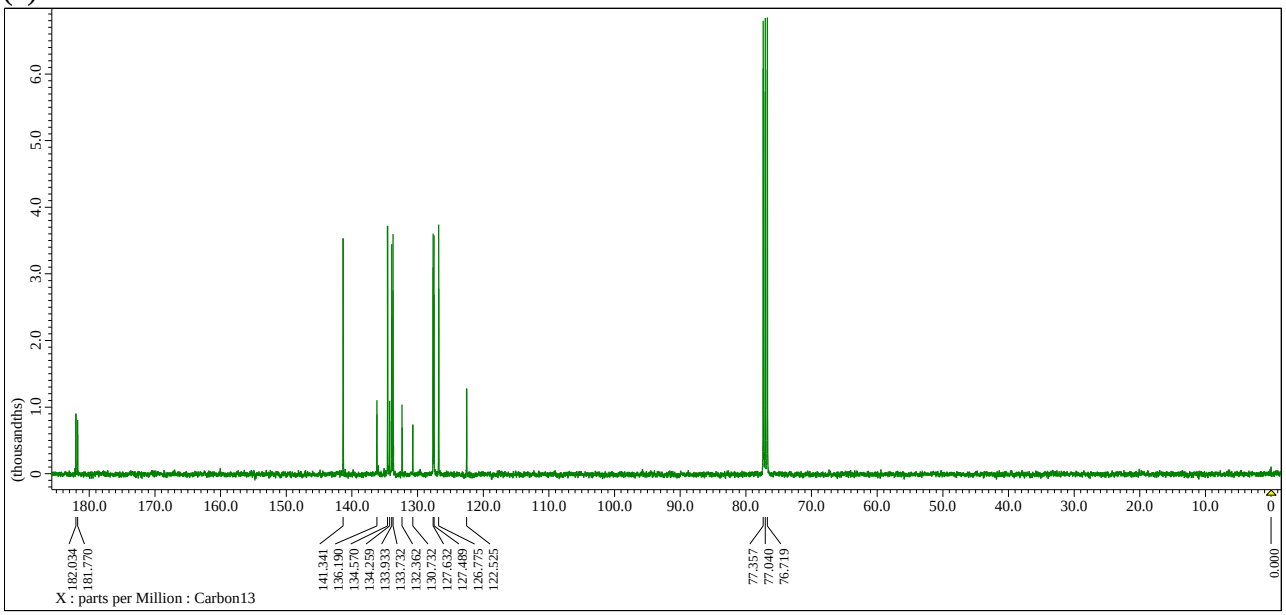

(b)

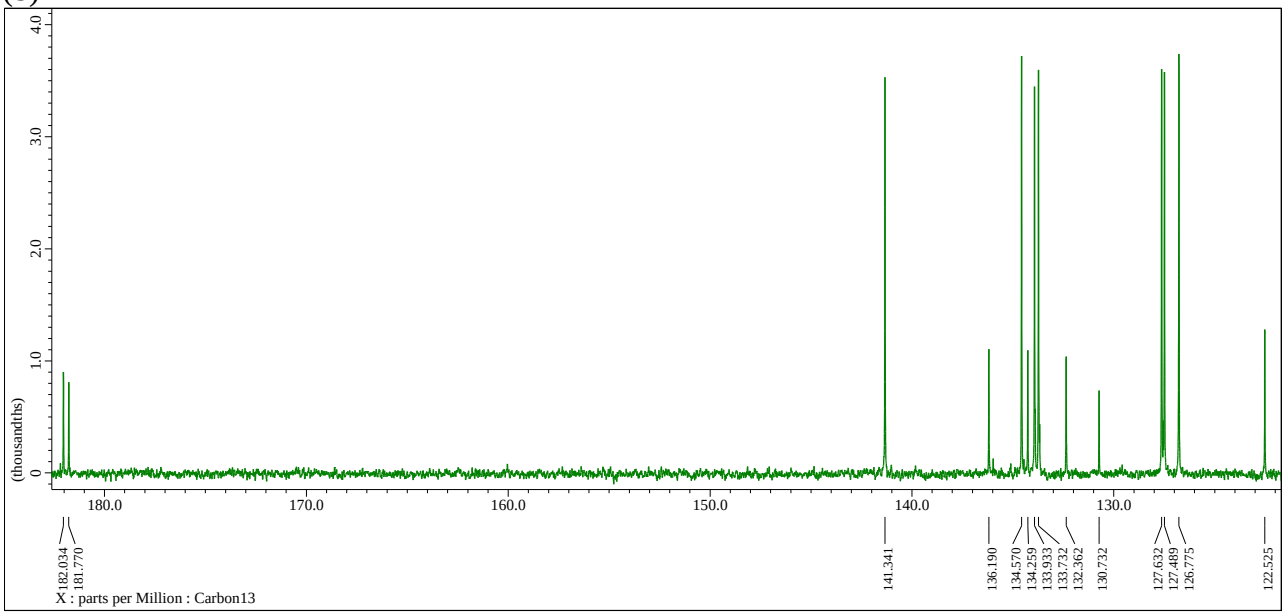

Fig. S19 ^{13}C NMR spectrum of **7**.

(a)

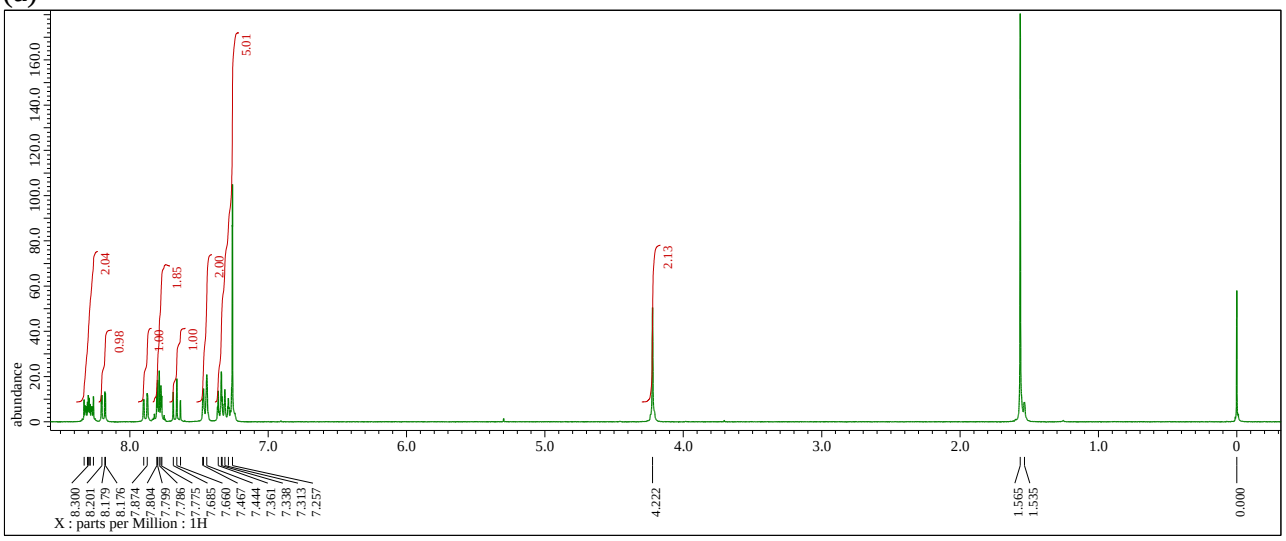

(b)

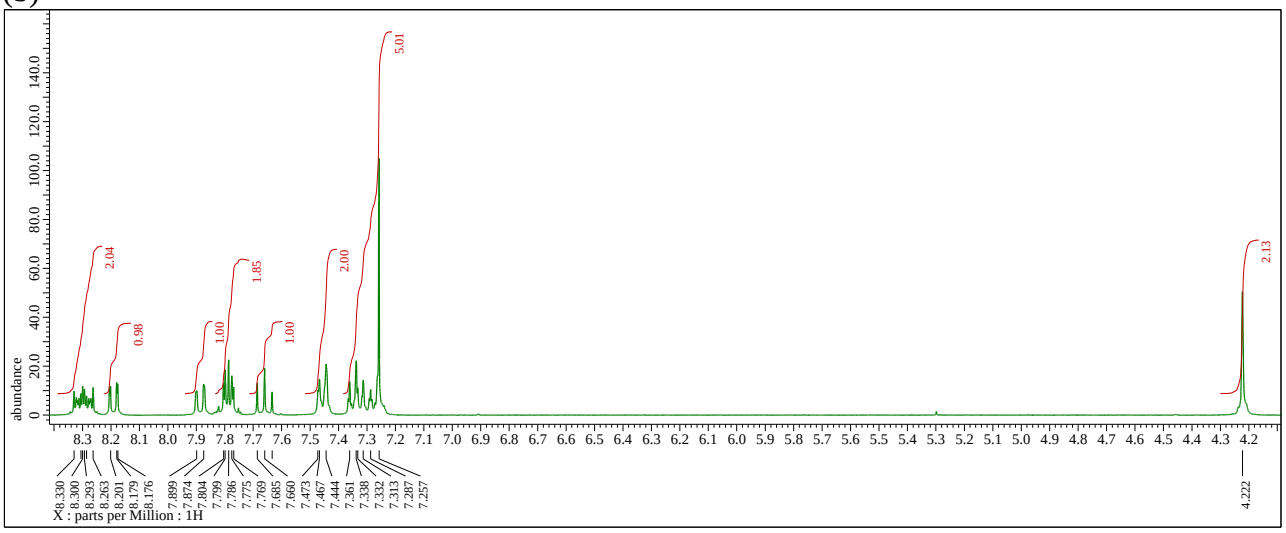

Fig. S20 ^{1}H NMR spectrum of **9**.

(a)

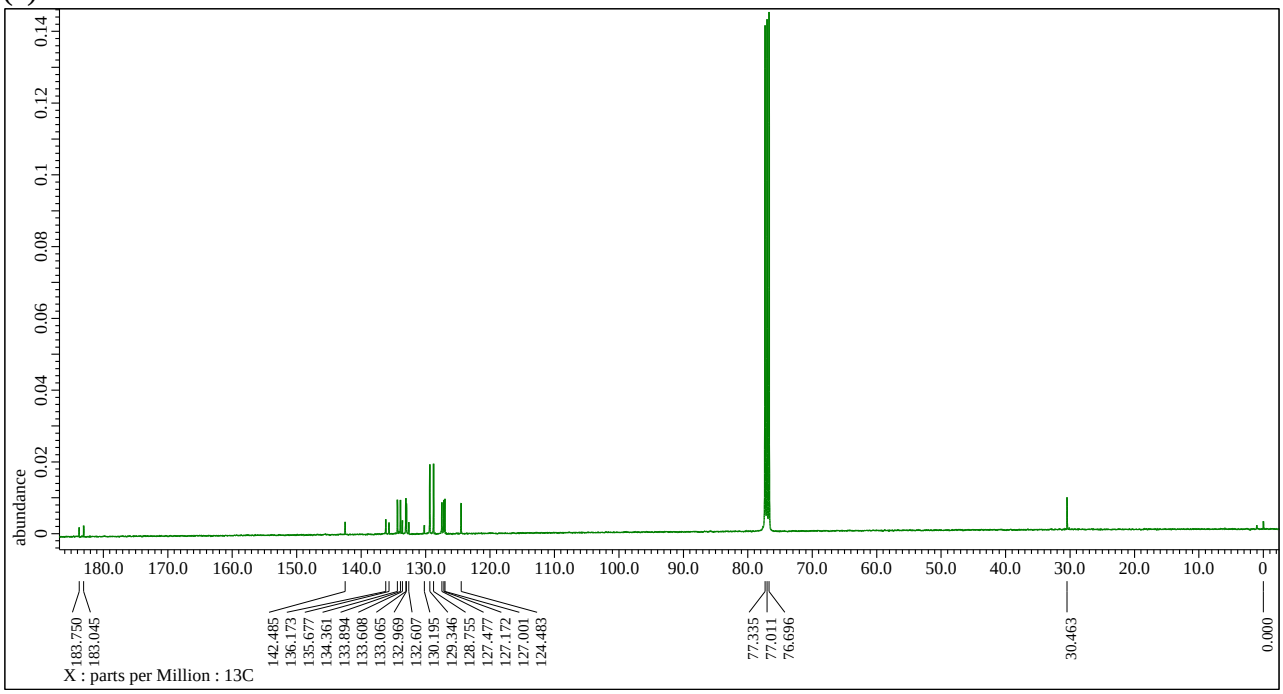

(b)

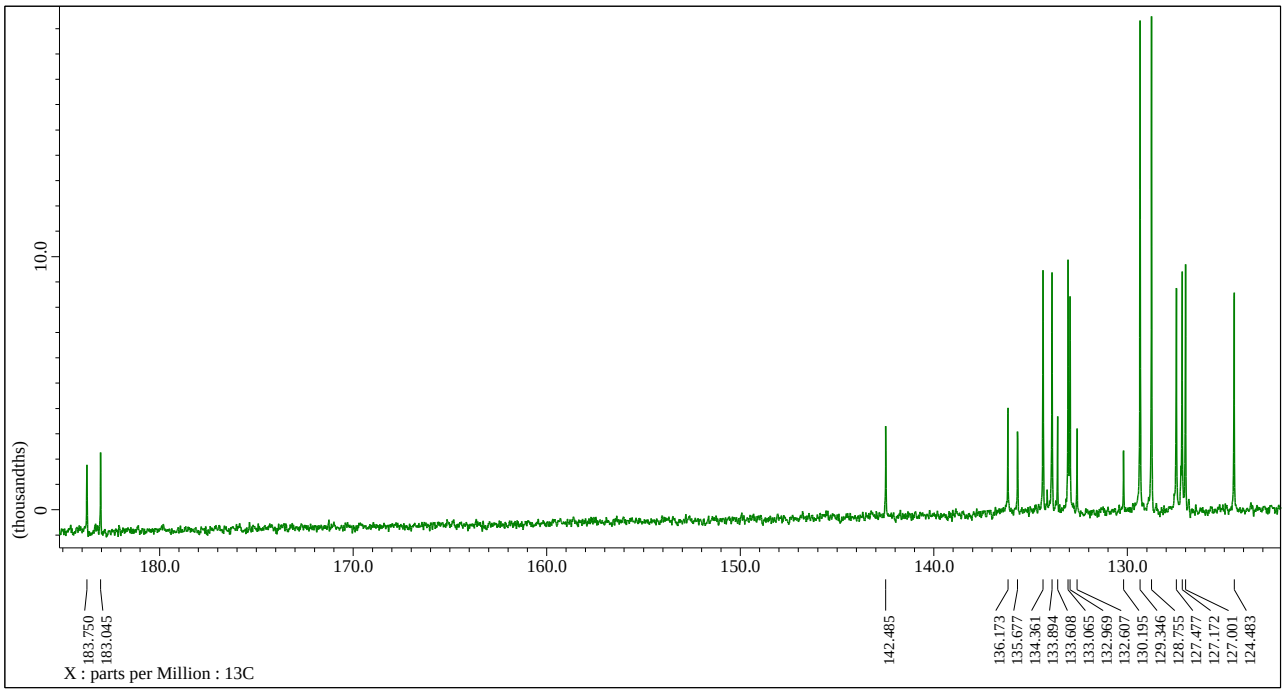

Fig. S21 ^{1}H NMR spectrum of **9**.

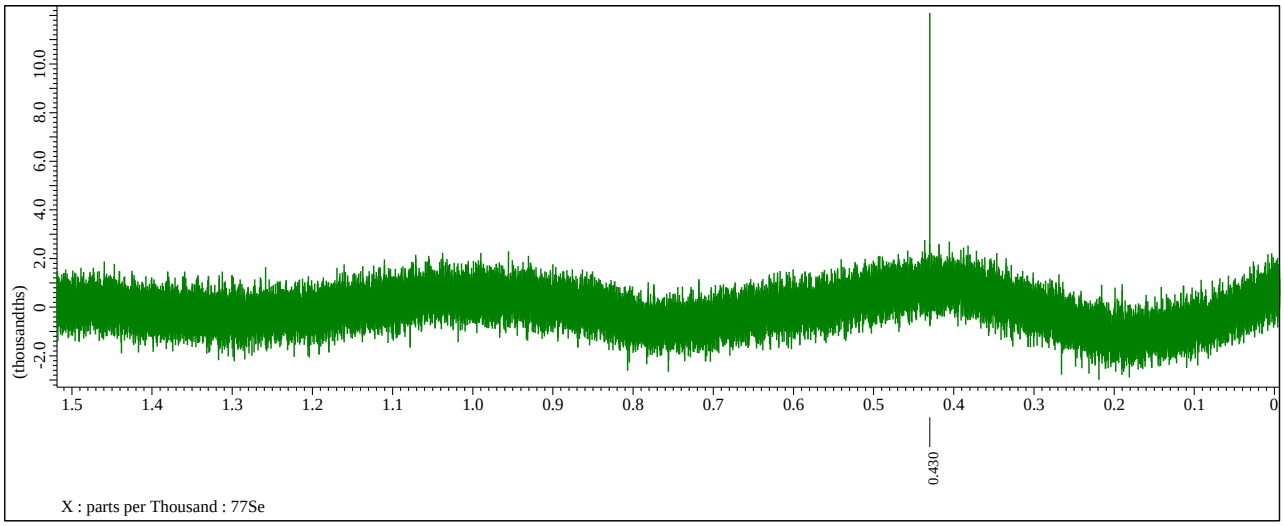

Fig. S22 ^{77}Se NMR spectrum of **9**.

Optimized structures given by Cartesian coordinates

Optimized structures given by Cartesian coordinates for examined molecules, together with the total energies calculated with the MP2/BSS-A or MP2/BSS-B methods of the Gaussian 09 program package. The BSS-A is the Sapporo-TZP + 1s1p for all atoms, implemented from the Sapporo Basis Set Factory. The BSS-B is the Sapporo-TZP with diffuse functions of the 1s1p type (Sapporo-TZP + 1s1p) for O and Se with Sapporo-DZP for C and H. The optimized structures were confirmed by the frequency analysis. All structures have all positive frequencies.

MP2/BSS-A
Adduct **1** (ATQSeI)
Symmetry C_s
Energy MP2 = −10004.9054879 au
Standard Orientation

8	0	-0.542499	-1.891984	0.000000
6	0	0.662614	-1.583886	0.000000
6	0	3.468605	-0.801198	0.000000
8	0	4.649265	-0.469228	0.000000
6	0	1.031428	-0.181769	0.000000
6	0	2.383228	0.212278	0.000000
6	0	1.717799	-2.607895	0.000000
6	0	3.069932	-2.230522	0.000000
6	0	0.000000	0.782359	0.000000
6	0	0.358057	2.134273	0.000000
6	0	1.696190	2.512649	0.000000
6	0	2.713664	1.561610	0.000000
1	0	-0.415523	2.888851	0.000000
1	0	1.941714	3.566679	0.000000
1	0	3.757964	1.842323	0.000000
6	0	1.367328	-3.960288	0.000000
6	0	2.360202	-4.930597	0.000000
6	0	3.707177	-4.557418	0.000000
6	0	4.060472	-3.214033	0.000000
1	0	0.318185	-4.223857	0.000000
1	0	2.090385	-5.978160	0.000000
1	0	4.476955	-5.317509	0.000000
1	0	5.095836	-2.900794	0.000000
34	0	-1.784439	0.138654	0.000000
53	0	-3.038281	2.367633	0.000000

MP2/BSS-A
Adduct **2** (ATQSeBr)
Symmetry C_s
Energy MP2 = −5659.461754 au
Standard Orientation

8	0	1.433924	-1.109604	0.000000
6	0	1.323771	0.133838	0.000000
6	0	0.964106	3.021424	0.000000
8	0	0.814128	4.238648	0.000000
6	0	0.000000	0.706330	0.000000
6	0	-0.198304	2.099445	0.000000
6	0	2.494959	1.017378	0.000000
6	0	2.319239	2.411360	0.000000
6	0	-1.092716	-0.184258	0.000000
6	0	-2.385622	0.351353	0.000000
6	0	-2.572070	1.729411	0.000000

6	0	-1.489594	2.609375	0.000000
1	0	-3.236627	-0.314010	0.000000
1	0	-3.581577	2.119512	0.000000
1	0	-1.627750	3.681991	0.000000
6	0	3.780618	0.470750	0.000000
6	0	4.886529	1.309921	0.000000
6	0	4.715568	2.697096	0.000000
6	0	3.438856	3.244802	0.000000
1	0	3.887351	-0.605769	0.000000
1	0	5.882949	0.888869	0.000000
1	0	5.580762	3.346492	0.000000
1	0	3.282272	4.315147	0.000000
34	0	-0.684241	-2.028598	0.000000
35	0	-2.914847	-2.834332	0.000000

MP2/BSS-A
Adduct **3** (ATQSeCl)
Symmetry C_s
Energy MP2 = −3546.4898225 au
Standard Orientation

8	0	-0.192048	-1.785484	0.000000
6	0	0.579622	-0.801807	0.000000
6	0	2.276400	1.560612	0.000000
8	0	2.994656	2.554730	0.000000
6	0	0.000000	0.515404	0.000000
6	0	0.797670	1.674177	0.000000
6	0	2.037551	-0.952619	0.000000
6	0	2.855129	0.190715	0.000000
6	0	-1.406363	0.595660	0.000000
6	0	-1.999961	1.863774	0.000000
6	0	-1.203980	3.004121	0.000000
6	0	0.189691	2.921845	0.000000
1	0	-3.076326	1.951642	0.000000
1	0	-1.683107	3.974554	0.000000
1	0	0.811386	3.806822	0.000000
6	0	2.609808	-2.227081	0.000000
6	0	3.991492	-2.362098	0.000000
6	0	4.807982	-1.227745	0.000000
6	0	4.242864	0.041408	0.000000
1	0	1.957482	-3.090107	0.000000
1	0	4.436995	-3.347822	0.000000
1	0	5.884071	-1.338649	0.000000
1	0	4.855052	0.933265	0.000000
34	0	-2.344732	-1.039251	0.000000
17	0	-4.385468	-0.146315	0.000000

MP2/BSS-A
Adduct **4** (ATQSeF)
Symmetry C_s
Energy MP2 = −3186.5288349 au
Standard Orientation

8	0	-1.216076	-1.363672	0.000000
6	0	-0.070435	-0.844130	0.000000
6	0	2.492743	0.527759	0.000000
8	0	3.579656	1.096450	0.000000
6	0	0.000000	0.581857	0.000000
6	0	1.218684	1.282376	0.000000
6	0	1.161459	-1.630217	0.000000

6	0	2.399724	-0.960348	0.000000
6	0	-1.235959	1.247696	0.000000
6	0	-1.245007	2.650536	0.000000
6	0	-0.037495	3.338105	0.000000
6	0	1.193318	2.668951	0.000000
1	0	-2.186683	3.179202	0.000000
1	0	-0.052673	4.420311	0.000000
1	0	2.129664	3.210661	0.000000
6	0	1.114405	-3.026442	0.000000
6	0	2.295745	-3.755543	0.000000
6	0	3.527876	-3.095917	0.000000
6	0	3.578797	-1.707483	0.000000
1	0	0.149214	-3.515255	0.000000
1	0	2.262191	-4.836753	0.000000
1	0	4.445492	-3.668843	0.000000
1	0	4.521375	-1.176587	0.000000
34	0	-2.762892	0.181403	0.000000
9	0	-3.844670	1.632681	0.000000

MP2/BSS-A
Adduct **5** (ATQSeH)
Symmetry C_s
Energy MP2 = −3186.5288349 au
Standard Orientation

8	0	-1.808363	-0.852878	0.000000
6	0	-0.585333	-0.697406	0.000000
6	0	2.322480	-0.347175	0.000000
8	0	3.539761	-0.193694	0.000000
6	0	0.000000	0.650878	0.000000
6	0	1.400830	0.818788	0.000000
6	0	0.326019	-1.863489	0.000000
6	0	1.718069	-1.698552	0.000000
6	0	-0.839419	1.782345	0.000000
6	0	-0.250882	3.053624	0.000000
6	0	1.129676	3.206680	0.000000
6	0	1.960777	2.091949	0.000000
1	0	-0.882521	3.932592	0.000000
1	0	1.553938	4.202161	0.000000
1	0	3.038220	2.182247	0.000000
6	0	-0.221445	-3.148846	0.000000
6	0	0.613172	-4.258337	0.000000
6	0	2.001144	-4.093679	0.000000
6	0	2.551612	-2.819078	0.000000
1	0	-1.298252	-3.250601	0.000000
1	0	0.187768	-5.253058	0.000000
1	0	2.647576	-4.961169	0.000000
1	0	3.622034	-2.663670	0.000000
34	0	-2.723814	1.618943	0.000000
1	0	-2.870476	3.073817	0.000000

MP2/BSS-A
Adduct **6** (ATQSeMe)
Symmetry C_s
Energy MP2 = −3126.6225686 au
Standard Orientation

8	0	-1.159585	-1.553485	0.000000
6	0	-0.070614	-0.974789	0.000000
6	0	2.527574	0.369576	0.000000

8	0	3.612935	0.942194	0.000000
6	0	0.000000	0.492177	0.000000
6	0	1.254258	1.137502	0.000000
6	0	1.192509	-1.747957	0.000000
6	0	2.438566	-1.107230	0.000000
6	0	-1.188196	1.260512	0.000000
6	0	-1.071369	2.657419	0.000000
6	0	0.171955	3.279764	0.000000
6	0	1.338491	2.526376	0.000000
1	0	-1.955314	3.276289	0.000000
1	0	0.222259	4.360934	0.000000
1	0	2.317507	2.984988	0.000000
6	0	1.129839	-3.143590	0.000000
6	0	2.300144	-3.890708	0.000000
6	0	3.542845	-3.250871	0.000000
6	0	3.612155	-1.864222	0.000000
1	0	0.156653	-3.615582	0.000000
1	0	2.249806	-4.971450	0.000000
1	0	4.451985	-3.837312	0.000000
1	0	4.560258	-1.343564	0.000000
34	0	-2.885886	0.427330	0.000000
6	0	-3.985041	2.025098	0.000000
1	0	-3.831170	2.622181	0.895408
1	0	-3.831170	2.622181	-0.895408
1	0	-5.006185	1.648113	0.000000

MP2/BSS-A
Adduct **7** (ATQBr)
Symmetry C_1
Energy MP2 = −3259.3824383 au
Standard Orientation

8	0	-0.269209	-2.009799	0.449992
6	0	0.256786	-0.930986	0.206062
6	0	1.646682	1.647634	0.082928
8	0	2.216258	2.731880	0.142825
6	0	-0.525135	0.329249	0.073557
6	0	0.158383	1.566251	0.059321
6	0	1.732344	-0.845549	0.048505
6	0	2.402218	0.382602	0.001029
6	0	-1.929459	0.359272	-0.010129
6	0	-2.611770	1.573828	-0.081502
6	0	-1.917938	2.777801	-0.066605
6	0	-0.532607	2.774358	-0.000415
1	0	-3.690560	1.560770	-0.150456
1	0	-2.463207	3.710788	-0.116292
1	0	0.041572	3.690385	-0.000824
6	0	2.463007	-2.034288	-0.020678
6	0	3.844952	-1.993605	-0.148991
6	0	4.511933	-0.766063	-0.194162
6	0	3.793802	0.419013	-0.113923
1	0	1.926358	-2.971976	0.027456
1	0	4.407317	-2.915716	-0.211525
1	0	5.589146	-0.739920	-0.290359
1	0	4.283951	1.382834	-0.140018
35	0	-3.012290	-1.172883	-0.082014

MP2/BSS-B
Adduct **8** ((ATQSe)$_2$)

Symmetry C_2
Energy MP2 = −6172.7811061 au
Standard Orientation

8	0	1.048729	-3.616961	-1.580885
6	0	0.404695	-4.106049	-0.642650
6	0	-1.064144	-5.262003	1.626999
8	0	-1.671025	-5.737243	2.587126
6	0	-0.441990	-3.244631	0.209909
6	0	-1.139341	-3.800268	1.316303
6	0	0.467981	-5.564882	-0.355574
6	0	-0.231171	-6.121937	0.739068
6	0	-0.549693	-1.853038	-0.065736
6	0	-1.343082	-1.053033	0.781134
6	0	-2.025583	-1.616020	1.870426
6	0	-1.929389	-2.987035	2.143404
1	0	-1.440015	0.014413	0.576086
1	0	-2.635184	-0.971001	2.507182
1	0	-2.451609	-3.446037	2.983781
6	0	1.248814	-6.392212	-1.185385
6	0	1.325277	-7.766291	-0.926392
6	0	0.626991	-8.322158	0.163995
6	0	-0.149029	-7.503533	0.994245
1	0	1.781385	-5.938269	-2.022440
1	0	1.928657	-8.408253	-1.571284
1	0	0.690320	-9.394056	0.361910
1	0	-0.698845	-7.909632	1.844646
34	0	0.408768	-1.095781	-1.551422
34	0	-0.408768	1.095781	-1.551422
6	0	0.549693	1.853038	-0.065736
6	0	0.441990	3.244631	0.209909
6	0	1.343082	1.053033	0.781134
6	0	-0.404695	4.106049	-0.642650
6	0	1.139341	3.800268	1.316303
6	0	2.025583	1.616020	1.870426
1	0	1.440015	-0.014413	0.576086
8	0	-1.048729	3.616961	-1.580885
6	0	-0.467981	5.564882	-0.355574
6	0	1.064144	5.262003	1.626999
6	0	1.929389	2.987035	2.143404
1	0	2.635184	0.971001	2.507182
6	0	0.231171	6.121937	0.739068
6	0	-1.248814	6.392212	-1.185385
8	0	1.671025	5.737243	2.587126
1	0	2.451609	3.446037	2.983781
6	0	0.149029	7.503533	0.994245
6	0	-1.325277	7.766291	-0.926392
1	0	-1.781385	5.938269	-2.022440
6	0	-0.626991	8.322158	0.163995
1	0	0.698845	7.909632	1.844646
1	0	-1.928657	8.408253	-1.571284
1	0	-0.690320	9.394056	0.361910

MP2/BSS-A
Adduct **II** (I) (2-C_6H_4(CHO)SeI)
Symmetry C_s
Energy MP2 = −9662.3973587 au
Standard Orientation

6	0	3.382532	-1.301716	0.000000
6	0	2.496937	-0.217938	0.000000

6	0	1.100248	-0.422686	0.000000
6	0	0.630134	-1.737453	0.000000
6	0	1.519818	-2.806300	0.000000
6	0	2.900351	-2.599815	0.000000
1	0	4.448046	-1.103919	0.000000
1	0	-0.434178	-1.923932	0.000000
1	0	1.125102	-3.814079	0.000000
1	0	3.580437	-3.440079	0.000000
6	0	3.017196	1.134466	0.000000
1	0	4.111152	1.256624	0.000000
8	0	2.278945	2.117984	0.000000
34	0	0.000000	1.127286	0.000000
53	0	-2.289536	0.027593	0.000000

MP2/BSS-A
Adduct **II** (Br) (2-C_6H_4(CHO)SeBr)
Symmetry C_s
Energy MP2 = −5316.9530657 au
Standard Orientation

6	0	0.400252	3.244377	0.000000
6	0	0.882434	1.929704	0.000000
6	0	0.000000	0.828866	0.000000
6	0	-1.373675	1.083846	0.000000
6	0	-1.840923	2.392889	0.000000
6	0	-0.963147	3.480750	0.000000
1	0	1.109282	4.063742	0.000000
1	0	-2.069960	0.258278	0.000000
1	0	-2.909433	2.565335	0.000000
1	0	-1.346168	4.491622	0.000000
6	0	2.298518	1.657377	0.000000
1	0	2.998290	2.504495	0.000000
8	0	2.722958	0.498257	0.000000
34	0	0.781623	-0.896049	0.000000
35	0	-1.216046	-2.146020	0.000000

MP2/BSS-A
Adduct **II** (Cl) (2-C_6H_4(CHO)SeCl)
Symmetry C_s
Energy MP2 = −3203.9811078 au
Standard Orientation

6	0	1.423980	2.492646	0.000000
6	0	1.276240	1.099715	0.000000
6	0	0.000000	0.499198	0.000000
6	0	-1.123590	1.330790	0.000000
6	0	-0.964923	2.711297	0.000000
6	0	0.302787	3.302605	0.000000
1	0	2.420934	2.916876	0.000000
1	0	-2.112979	0.898577	0.000000
1	0	-1.847602	3.337680	0.000000
1	0	0.402175	4.379026	0.000000
6	0	2.415153	0.220176	0.000000
1	0	3.425141	0.650397	0.000000
8	0	2.260631	-1.006729	0.000000
34	0	-0.055876	-1.389844	0.000000
17	0	-2.261812	-1.577211	0.000000

MP2/BSS-A
Adduct **II** (F) (2-C_6H_4(CHO)SeF)
Symmetry C_s
Energy MP2 = −2844.0198113 au
Standard Orientation

6	0	2.220646	1.442493	0.000000
6	0	1.404687	0.300607	0.000000
6	0	0.000000	0.404522	0.000000
6	0	-0.585611	1.677351	0.000000
6	0	0.230653	2.797980	0.000000
6	0	1.630402	2.690896	0.000000
1	0	3.297955	1.330385	0.000000
1	0	-1.660991	1.771823	0.000000
1	0	-0.226391	3.779154	0.000000
1	0	2.240051	3.583706	0.000000
6	0	1.900507	-1.038807	0.000000
1	0	2.974740	-1.247289	0.000000
8	0	1.086929	-1.982891	0.000000
34	0	-0.976176	-1.185912	0.000000
9	0	-2.548724	-0.298210	0.000000

MP2/BSS-A
Adduct **II** (H) (2-C_6H_4(CHO)SeH)
Symmetry C_s
Energy MP2 = −2744.8967293 au
Standard Orientation

6	0	2.411345	0.095461	0.000000
6	0	1.112811	-0.427814	0.000000
6	0	0.000000	0.431596	0.000000
6	0	0.231489	1.811200	0.000000
6	0	1.524827	2.319917	0.000000
6	0	2.626755	1.464224	0.000000
1	0	3.247321	-0.594543	0.000000
1	0	-0.607652	2.494897	0.000000
1	0	1.670887	3.392247	0.000000
1	0	3.631398	1.863470	0.000000
6	0	0.963112	-1.885380	0.000000
1	0	1.910991	-2.452310	0.000000
8	0	-0.111171	-2.465914	0.000000
34	0	-1.760668	-0.262238	0.000000
1	0	-2.322901	1.084438	0.000000

MP2/BSS-A
Adduct **II** (Me) (2-C_6H_4(CHO)SeMe)
Symmetry C_s
Energy MP2 = −2784.1168018 au
Standard Orientation

6	0	2.173328	1.497976	0.000000
6	0	1.409722	0.325866	0.000000
6	0	0.000000	0.388237	0.000000
6	0	-0.595210	1.655371	0.000000
6	0	0.176479	2.813342	0.000000
6	0	1.568302	2.745270	0.000000
1	0	3.253787	1.409662	0.000000
1	0	-1.670177	1.753807	0.000000
1	0	-0.319113	3.775687	0.000000
1	0	2.163733	3.647580	0.000000
6	0	2.135121	-0.946576	0.000000

1	0	3.236194	-0.852349	0.000000
8	0	1.603261	-2.045825	0.000000
34	0	-1.018786	-1.204524	0.000000
6	0	-2.781340	-0.403739	0.000000
1	0	-2.950898	0.189528	0.894986
1	0	-2.950898	0.189528	-0.894986
1	0	-3.468420	-1.247521	0.000000

MP2/BSS-A
Adduct **IV** (I) (2-$C_6H_4(CH_2OMe)SeI$)
Symmetry C_1
Energy MP2 = −9702.80037 au
Standard Orientation

6	0	2.221619	0.314363	-0.480893
6	0	0.915986	0.528522	-0.009842
6	0	0.545451	1.785778	0.464825
6	0	1.463660	2.832179	0.457748
6	0	2.760279	2.630958	-0.007111
6	0	3.131564	1.369774	-0.463074
1	0	-0.458250	1.948740	0.832298
1	0	1.161720	3.803849	0.825956
1	0	3.474859	3.442733	-0.006530
1	0	4.140529	1.195225	-0.818504
6	0	2.612509	-1.042403	-0.985606
1	0	2.107502	-1.259988	-1.928593
1	0	3.695352	-1.092507	-1.143770
8	0	2.191628	-2.070224	-0.096574
6	0	2.862761	-2.003520	1.154181
1	0	3.940890	-2.122261	1.016688
1	0	2.667906	-1.053905	1.658470
1	0	2.479208	-2.820498	1.757544
34	0	-0.249253	-0.990423	-0.000778
53	0	-2.478323	0.183036	-0.041054

MP2/BSS-A
Adduct **IV** (Br) (2-$C_6H_4(CH_2OMe)SeBr$)
Symmetry C_1
Energy MP2 = −5357.3543941 au
Standard Orientation

6	0	1.890539	0.227868	-0.451003
6	0	0.586287	0.524093	-0.025421
6	0	0.274487	1.807185	0.421517
6	0	1.256092	2.794622	0.435784
6	0	2.554054	2.509485	0.020687
6	0	2.864026	1.223363	-0.411283
1	0	-0.730572	2.033505	0.747983
1	0	1.002126	3.787584	0.782743
1	0	3.316466	3.276211	0.040795
1	0	3.871945	0.983915	-0.730001
6	0	2.196704	-1.154896	-0.940459
1	0	1.756591	-1.319410	-1.925825
1	0	3.278038	-1.315258	-1.003014
8	0	1.594661	-2.135757	-0.101152
6	0	2.183796	-2.166693	1.194053
1	0	3.239988	-2.437468	1.122649
1	0	2.090807	-1.199080	1.692509
1	0	1.648311	-2.921648	1.761114
34	0	-0.676337	-0.912123	-0.048237

35	0	-2.630613	0.360564	-0.042941

MP2/BSS-A
Adduct **IV** (Cl) (2-$C_6H_4(CH_2OMe)SeCl$)
Symmetry C_1
Energy MP2 = −3244.3814962 au
Standard Orientation

6	0	1.503734	-0.084997	-0.437079
6	0	0.307355	0.525134	-0.031382
6	0	0.313107	1.850064	0.402579
6	0	1.507686	2.565493	0.424255
6	0	2.701380	1.966353	0.030804
6	0	2.692142	0.639478	-0.389005
1	0	-0.607974	2.321022	0.714468
1	0	1.501719	3.593874	0.760770
1	0	3.628298	2.522755	0.058309
1	0	3.614288	0.156889	-0.691555
6	0	1.458030	-1.503028	-0.917933
1	0	1.024166	-1.555909	-1.918262
1	0	2.460063	-1.943173	-0.941064
8	0	0.589162	-2.282035	-0.099563
6	0	1.115225	-2.472442	1.210165
1	0	2.054000	-3.028878	1.161200
1	0	1.285161	-1.515443	1.708529
1	0	0.376150	-3.044883	1.761677
34	0	-1.273227	-0.548608	-0.071396
17	0	-2.726552	1.087434	-0.067325

MP2/BSS-A
Adduct **IV** (F) (2-$C_6H_4(CH_2OMe)SeF$)
Symmetry C_1
Energy MP2 = −2884.4167093 au
Standard Orientation

6	0	-1.082634	0.757781	-0.391230
6	0	-0.432713	-0.431941	-0.042570
6	0	-1.173457	-1.547022	0.350268
6	0	-2.562702	-1.464155	0.394642
6	0	-3.216761	-0.278598	0.065530
6	0	-2.470708	0.831602	-0.320434
1	0	-0.666662	-2.464549	0.611582
1	0	-3.135070	-2.330487	0.699202
1	0	-4.295385	-0.218317	0.115000
1	0	-2.966802	1.760242	-0.577879
6	0	-0.227110	1.894479	-0.857119
1	0	0.072086	1.750711	-1.896974
1	0	-0.738971	2.856367	-0.761573
8	0	0.998119	1.907348	-0.121669
6	0	0.807187	2.349256	1.222361
1	0	0.463088	3.385065	1.224889
1	0	0.082341	1.717578	1.739804
1	0	1.772241	2.277325	1.713130
34	0	1.463845	-0.479657	-0.113853
9	0	1.534539	-2.261422	-0.061279

MP2/BSS-A
Adduct **IV** (H) (2-$C_6H_4(CH_2OMe)SeH$)

Symmetry C_1
Energy MP2 = −2785.3007888 au
Standard Orientation

6	0	-0.733314	0.678964	-0.466302
6	0	-0.368427	-0.607804	-0.045847
6	0	-1.350666	-1.498250	0.394285
6	0	-2.689745	-1.120876	0.404640
6	0	-3.060386	0.157214	-0.005645
6	0	-2.078576	1.047430	-0.428299
1	0	-1.068909	-2.487407	0.731838
1	0	-3.439411	-1.824033	0.742979
1	0	-4.099054	0.458181	0.011195
1	0	-2.353318	2.047457	-0.743393
6	0	0.310057	1.642855	-0.955256
1	0	0.778346	1.261916	-1.864629
1	0	-0.158968	2.608330	-1.179778
8	0	1.374988	1.814812	-0.034162
6	0	0.932877	2.373663	1.190113
1	0	0.449181	3.341458	1.024361
1	0	0.230358	1.710870	1.702072
1	0	1.814486	2.511626	1.808941
34	0	1.468580	-1.107643	-0.070060
1	0	1.144759	-2.526212	-0.104401

MP2/BSS-A
Adduct **IV** (Me) (2-$C_6H_4(CH_2OMe)SeMe$)
Symmetry C_1
Energy MP2 = −2824.520911 au
Standard Orientation

6	0	-1.206718	0.165240	-0.469296
6	0	-0.102302	-0.586867	-0.032451
6	0	-0.297187	-1.898725	0.408466
6	0	-1.569994	-2.463857	0.409853
6	0	-2.667554	-1.722767	-0.016927
6	0	-2.475594	-0.412364	-0.444910
1	0	0.538720	-2.487759	0.758494
1	0	-1.699624	-3.481775	0.753906
1	0	-3.658457	-2.156153	-0.010852
1	0	-3.321979	0.178445	-0.775980
6	0	-1.024247	1.570776	-0.967025
1	0	-0.392170	1.575745	-1.856939
1	0	-2.001916	1.994618	-1.227162
8	0	-0.358233	2.408659	-0.036298
6	0	-1.082605	2.540020	1.172930
1	0	-2.085679	2.937337	0.986621
1	0	-1.173647	1.581801	1.691222
1	0	-0.528988	3.235566	1.796749
34	0	1.616650	0.223468	-0.049811
6	0	2.680020	-1.393937	-0.052043
1	0	3.698051	-1.073792	-0.263167
1	0	2.659327	-1.888387	0.914915
1	0	2.343207	-2.067921	-0.835436

Appendix

QTAIM Dual Functional Analysis (QTAIM-DFA)

The bond critical point (BCP; ∗) is an important concept in QTAIM. The BCP of $(\omega, \sigma) = (3, -1)$[SA1] is a point along the bond path (BP) at the interatomic surface, where charge density $\rho(\boldsymbol{r})$ reaches a minimum. It is donated by $\rho_b(\boldsymbol{r}_c)$, so are other QTAIM functions, such as the total electron energy densities $H_b(\boldsymbol{r}_c)$, potential energy densities $V_b(\boldsymbol{r}_c)$ and kinetic energy densities $G_b(\boldsymbol{r}_c)$ at the BCPs. A chemical bond or interaction between A and B is denoted by A–B, which corresponds to the BP between A and B in QTAIM. We will use A–B for BP, where the asterisk emphasizes the presence of a BCP in A–B.

The sign of the Laplacian $\rho_b(\boldsymbol{r}_c)$ ($\nabla^2\rho_b(\boldsymbol{r}_c)$) indicates that $\rho_b(\boldsymbol{r}_c)$ is depleted or concentrated with respect to its surrounding, since $\nabla^2\rho_b(\boldsymbol{r}_c)$ is the second derivative of $\rho_b(\boldsymbol{r}_c)$. $\rho_b(\boldsymbol{r}_c)$ is locally depleted relative to the average distribution around $\boldsymbol{r}_c$ if $\nabla^2\rho_b(\boldsymbol{r}_c) > 0$, but it is concentrated when $\nabla^2\rho_b(\boldsymbol{r}_c) < 0$. Total electron energy densities at BCPs ($H_b(\boldsymbol{r}_c)$) must be a more appropriate measure for weak interactions on the energy basis.[SA1–SA8] $H_b(\boldsymbol{r}_c)$ are the sum of kinetic energy densities ($G_b(\boldsymbol{r}_c)$) and potential energy densities ($V_b(\boldsymbol{r}_c)$) at BCPs, as shown in eqn (SA1). Electrons at BCPs are stabilized when $H_b(\boldsymbol{r}_c) < 0$, therefore, interactions exhibit the covalent nature in this region, whereas they exhibit no covalency if $H_b(\boldsymbol{r}_c) > 0$, due to the destabilization of electrons at BCPs under the conditions.[SA1] Eqns (SA2) and (SA2') represent the relations between $\nabla^2\rho_b(\boldsymbol{r}_c)$ and $H_b(\boldsymbol{r}_c)$, together with $G_b(\boldsymbol{r}_c)$ and $V_b(\boldsymbol{r}_c)$, which are closely related to the virial theorem.

$$H_b(\boldsymbol{r}_c) = G_b(\boldsymbol{r}_c) + V_b(\boldsymbol{r}_c) \quad \text{(SA1)}$$

$$(\hbar^2/8m)\nabla^2\rho_b(\boldsymbol{r}_c) = H_b(\boldsymbol{r}_c) - V_b(\boldsymbol{r}_c)/2 \quad \text{(SA2)}$$

$$= G_b(\boldsymbol{r}_c) + V_b(\boldsymbol{r}_c)/2 \quad \text{(SA2')}$$

Interactions are classified by the signs of $\nabla^2\rho_b(\boldsymbol{r}_c)$ and $H_b(\boldsymbol{r}_c)$. Interactions in the region of $\nabla^2\rho_b(\boldsymbol{r}_c) < 0$ are called shared-shell (SS) interactions and they are closed-shell (CS) interactions for $\nabla^2\rho_b(\boldsymbol{r}_c) > 0$. $H_b(\boldsymbol{r}_c)$ must be negative when $\nabla^2\rho_b(\boldsymbol{r}_c) < 0$, since $H_b(\boldsymbol{r}_c)$ are larger than $(\hbar^2/8m)\nabla^2\rho_b(\boldsymbol{r}_c)$ by $V_b(\boldsymbol{r}_c)/2$ with negative $V_b(\boldsymbol{r}_c)$ at all BCPs (eqn (S2)). Consequently, $\nabla^2\rho_b(\boldsymbol{r}_c) < 0$ and $H_b(\boldsymbol{r}_c) < 0$ for the SS interactions. The CS interactions are especially called *pure* CS interactions for $H_b(\boldsymbol{r}_c) > 0$ and $\nabla^2\rho_b(\boldsymbol{r}_c) > 0$, since electrons at BCPs are depleted and destabilized under the conditions.[SA1a] Electrons in the intermediate region between SS and *pure* CS, which belong to CS, are locally depleted but stabilized at BCPs, since $\nabla^2\rho_b(\boldsymbol{r}_c) > 0$ but $H_b(\boldsymbol{r}_c) < 0$.[SA1a] We call the interactions in this region *regular* CS,[SA4,SA5] when it is necessary to distinguish from *pure* CS. The role of $\nabla^2\rho_b(\boldsymbol{r}_c)$ in the classification can be replaced by $H_b(\boldsymbol{r}_c) - V_b(\boldsymbol{r}_c)/2$, since $(\hbar^2/8m)\nabla^2\rho_b(\boldsymbol{r}_c) = H_b(\boldsymbol{r}_c) - V_b(\boldsymbol{r}_c)/2$ (eqn (S2)). Scheme S1 summarizes the classification.

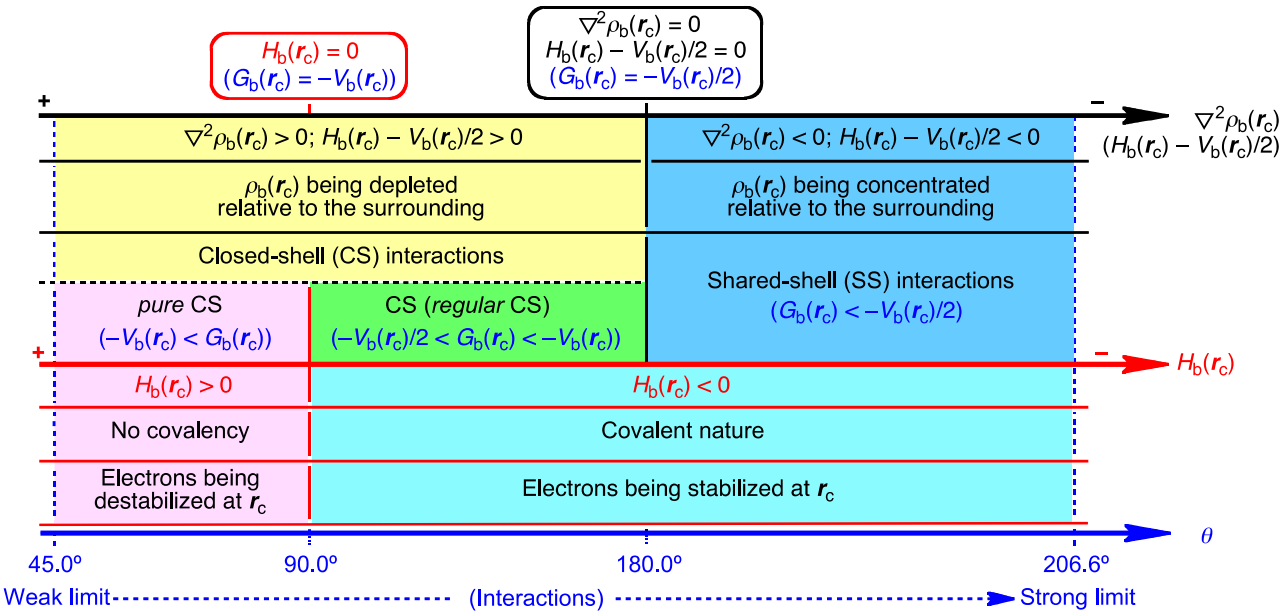

Scheme SA1. Classification of interactions by the signs of $\nabla^2\rho_b(r_c)$ and $H_b(r_c)$, together with $G_b(r_c)$ and $V_b(r_c)$.

We proposed QTAIM-DFA by plotting $H_b(r_c)$ versus $H_b(r_c) - V_b(r_c)/2$ (= $(\hbar^2/8m)\nabla^2\rho_b(r_c)$),[SA4a] after the proposal of $H_b(r_c)$ versus $\nabla^2\rho_b(r_c)$.[SA4b] Both axes in the plot of the former are given in energy unit, therefore, distances on the (x, y) (= ($H_b(r_c) - V_b(r_c)/2$, $H_b(r_c)$)) plane can be expressed in the energy unit, which provides an analytical development. QTAIM-DFA incorporates the classification of interactions by the signs of $\nabla^2\rho_b(r_c)$ and $H_b(r_c)$. Scheme S2 summarizes the QTAIM-DFA treatment. Interactions of *pure* CS appear in the first quadrant, those of *regular* CS in the fourth quadrant and SS interactions do in the third quadrant. No interactions appear in the second one.

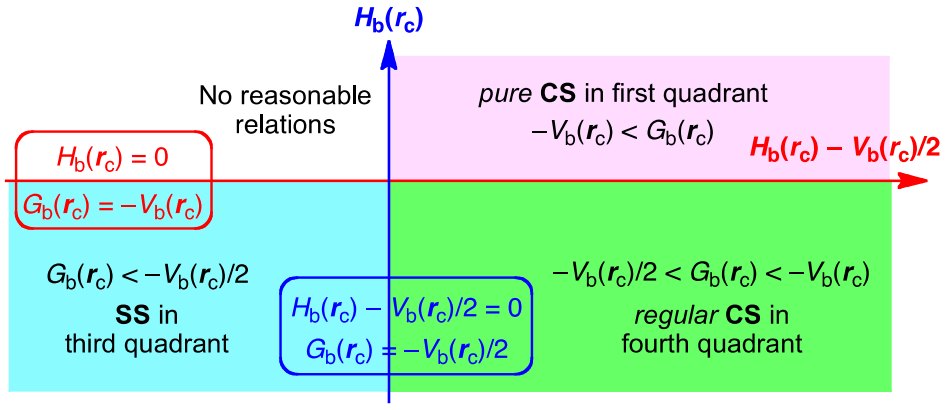

Scheme SA2. QTAIM-DFA: Plot of $H_b(r_c)$ versus $H_b(r_c) - V_b(r_c)/2$ for Weak to Strong Interactions.

In our treatment, data for perturbed structures around fully optimized structures are also employed for the plots, together with the fully optimized ones (see Fig. S1).[SA4–SA8] We proposed the concept of the "dynamic nature of interaction" originated from the perturbed structures. The behaviour of interactions at the fully optimized structures corresponds to "the static nature of interactions", whereas that containing perturbed structures exhibit the "dynamic nature of interaction" as explained below.

The method to generate the perturbed structures is discussed later. Plots of $H_b(\boldsymbol{r}_c)$ versus $H_b(\boldsymbol{r}_c) - V_b(\boldsymbol{r}_c)/2$ are analysed employing the polar coordinate (R, θ) representation with (θ_p, κ_p) parameters.[SA4a,SA5–SA8] Fig. S1 explains the treatment. R in (R, θ) is defined by eqn (S3) and given in the energy unit. Indeed, R does not correspond to the usual interaction energy, but it does to the local energy at BCP, expressed by $[(H_b(\boldsymbol{r}_c))^2 + (H_b(\boldsymbol{r}_c) - V_b(\boldsymbol{r}_c)/2)^2]^{1/2}$ in the plot (cf: eqn (S3)), where R = 0 for the enough large interaction distance. The plots show a spiral stream, as a whole. θ in (R, θ) defined by eqn (S4), measured from the y-axis, controls the spiral stream of the plot. Each plot for an interaction shows a specific curve, which provides important information of the interaction (see Fig. S1). The curve is expressed by θ_p and κ_p. While θ_p, defined by eqn (S5) and measured from the y-direction, corresponds to the tangent line of a plot, where θ_p is calculated employing data of the perturbed structures with a fully-optimized structure and κ_p is the curvature of the plot (eqn (S6)). While (R, θ) correspond to the static nature, (θ_p, κ_p) represent the dynamic nature of interactions. We call (R, θ) and (θ_p, κ_p) QTAIM-DFA parameters, whereas $\rho_b(\boldsymbol{r}_c)$, $\nabla^2\rho_b(\boldsymbol{r}_c)$, $G_b(\boldsymbol{r}_c)$, $V_b(\boldsymbol{r}_c)$, $H_b(\boldsymbol{r}_c)$ and $H_b(\boldsymbol{r}_c) - V_b(\boldsymbol{r}_c)/2$ belong to QTAIM functions. $k_b(\boldsymbol{r}_c)$, defined by eqn (S7), is an QTAIM function but it will be treated as if it were an QTAIM-DFA parameter, if suitable.

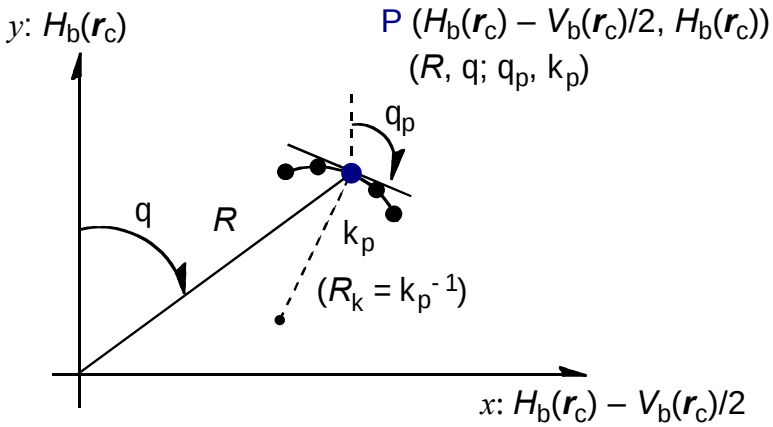

Fig. SA1 Polar (R, θ) coordinate representation of $H_b(\boldsymbol{r}_c)$ versus $H_b(\boldsymbol{r}_c) - V_b(\boldsymbol{r}_c)/2$, with ($\theta_p$, κ_p) parameters.

$$R = (x^2 + y^2)^{1/2} \quad \text{(SA3)}$$

$$\theta = 90^o - \tan^{-1}(y/x) \quad \text{(SA4)}$$

$$\theta_p = 90^o - \tan^{-1}(dy/dx) \quad \text{(SA5)}$$

$$\kappa_p = |d^2y/dx^2| / [1 + (dy/dx)^2]^{3/2} \quad \text{(SA6)}$$

$$k_b(\boldsymbol{r}_c) = V_b(\boldsymbol{r}_c)/G_b(\boldsymbol{r}_c) \quad \text{(SA7)}$$

where $(x, y) = (H_b(\boldsymbol{r}_c) - V_b(\boldsymbol{r}_c)/2, H_b(\boldsymbol{r}_c))$

Criteria for Classification of Interactions: Behaviour of Typical Interactions Elucidated by QTAIM-DFA

$H_b(\boldsymbol{r}_c)$ are plotted versus $H_b(\boldsymbol{r}_c) - V_b(\boldsymbol{r}_c)/2$ for typical interactions in vdW (van der Waals interactions), HBs (hydrogen bonds), CT-MCs (molecular complexes through charge transfer), X_3^- (trihalide ions), CT-TBPs (trigonal bipyramidal adducts through charge-transfer), Cov-w (weak covalent bonds) and Cov-s (strong covalent bonds).[SA4–SA8] Rough criteria are obtained by applying QTAIM-DFA, after the analysis of the plots for the typical interactions according to eqns (S3)–(S7). Scheme S3 shows the rough criteria, which are accomplished by the θ and θ_p values, together with the values of $k_b(\boldsymbol{r}_c)$. The criteria will be employed to discuss the nature of interactions in question, as a reference.

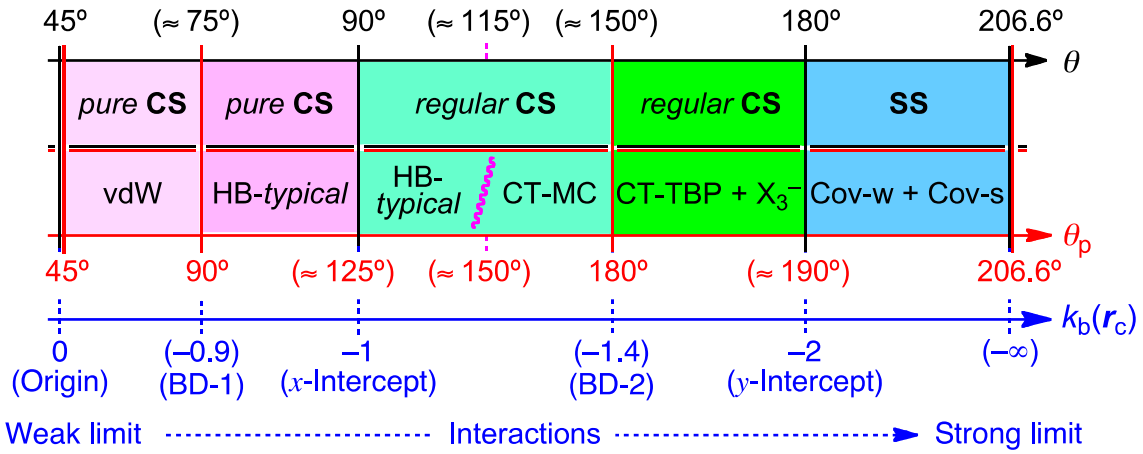

Scheme SA3. Rough classification and characterization of interactions by θ and θ_p, together with $k_b(\boldsymbol{r}_c)$ ($= V_b(\boldsymbol{r}_c)/G_b(\boldsymbol{r}_c)$).

Characterization of interactions

The characterization of interactions is explained employing $[^1Cl\text{-}^2Cl\text{-}^3Cl]^-$. The wide range of the perturbed structures were generated by partially optimizing $r(^2Cl\text{-}^3Cl)$ in $[^1Cl\text{-}^2Cl\text{-}^3Cl]^-$, assuming the $C_{\infty v}$ symmetry, with $r(^1Cl\text{-}^2Cl)$ being fixed in the wide range. The partial optimization method is called POM.[SA4b,SA5] The QTAIM functions, such as $V_b(\boldsymbol{r}_c)$, $G_b(\boldsymbol{r}_c)$, $H_b(\boldsymbol{r}_c)$, $H_b(\boldsymbol{r}_c) - V_b(\boldsymbol{r}_c)/2$ are calculated at BCPs for the wide varieties of the perturbed structures of $[^1Cl\text{-}^2Cl\text{-}^3Cl]^-$. $H_b(\boldsymbol{r}_c) - V_b(\boldsymbol{r}_c)/2$ and $H_b(\boldsymbol{r}_c)$ are plotted versus the interaction distances $r(^1Cl\text{-}^2Cl)$ in the perturbed structures of $[^1Cl\text{-}^2Cl\text{-}^3Cl]^-$, in the wide range. Fig. S2 shows the plots. Each plot is analysed using a regression curve of the ninth function and the first derivative of each regression curve is obtained. As shown in Fig. S2, the maximum value of $H_b(\boldsymbol{r}_c)$ ($d(H_b(\boldsymbol{r}_c)/dr = 0$) is defined as the borderline between vdW and t-HB interactions. Similarly, the maximum value of $H_b(\boldsymbol{r}_c) - V_b(\boldsymbol{r}_c)/2$ ($d(H_b(\boldsymbol{r}_c) - V_b(\boldsymbol{r}_c)/2)/dr = 0$) does to the borderline between CT-MC and CT-TBP. However, it seems difficult to find a characteristic point corresponding to the borderline between *t*-HB and CT-MC in nature. Therefore, the borderline

is tentatively given by $\theta_p = 150^o$ based on the expectation form the experimental results, where θ_p is defined by $[90^o - \tan^{-1}[d\mathit{H}_b(\boldsymbol{r}_c)/d(\mathit{H}_b(\boldsymbol{r}_c) - \mathit{V}_b(\boldsymbol{r}_c)/2)]]$ in the plot of $\mathit{H}_b(\boldsymbol{r}_c)$ versus $\mathit{H}_b(\boldsymbol{r}_c) - \mathit{V}_b(\boldsymbol{r}_c)/2$. The proposed classification and characterization of interactions, by means of the QTAIM functions of $\mathit{H}_b(\boldsymbol{r}_c)$, $\mathit{H}_b(\boldsymbol{r}_c) - \mathit{V}_b(\boldsymbol{r}_c)/2$, $\mathit{G}_b(\boldsymbol{r}_c)$ and/or $\mathit{V}_b(\boldsymbol{r}_c)$, are summarized in Table S1. The plot of $\mathit{H}_b(\boldsymbol{r}_c) - \mathit{V}_b(\boldsymbol{r}_c)/2$ versus w in Fig. S2 is essentially the same as that of $\nabla^2\rho_b(\boldsymbol{r}_c)$ versus d(H---F) in X–H---F–Y, presented by Espinosa and co-workers.[SA9]

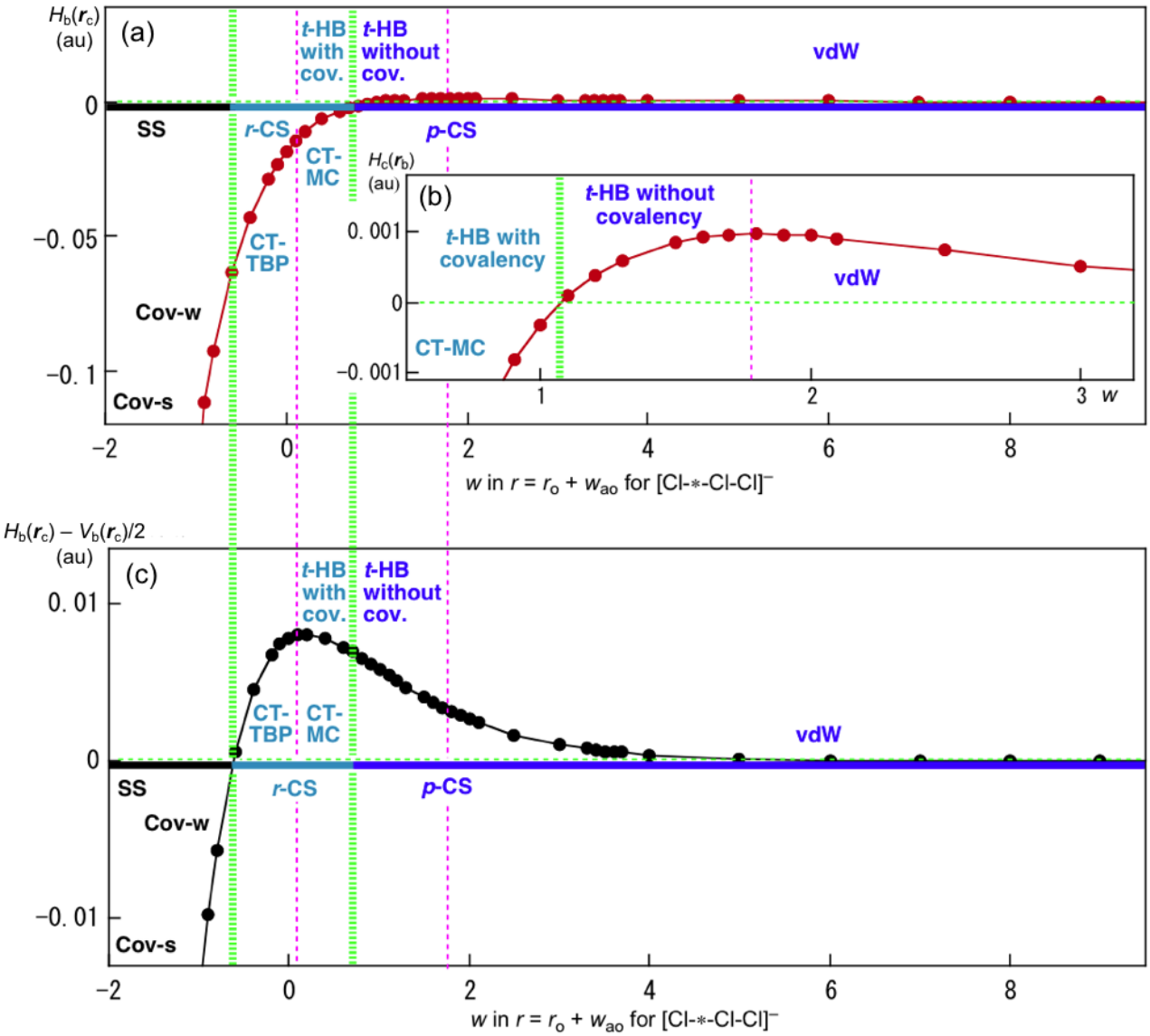

Fig. SA2 Plot of $\mathit{H}_b(\boldsymbol{r}_c)$ versus w in $r(^1\text{Cl-}^2\text{Cl}) = r_o(^1\text{Cl-}^2\text{Cl}) + wa_o$ for $^1\text{Cl-}^2\text{Cl-}^3\text{Cl}^-$ (a) with the magnified picture of (a) (b) and that of $\mathit{H}_b(\boldsymbol{r}_c) - \mathit{V}_b(\boldsymbol{r}_c)/2$ versus w (c). Typical hydrogen bonds without covalency and typical hydrogen bonds with covalency are abbreviated as *t*-HB without cov. and *t*-HB with cov., respectively, whereas Cov-w and Cov-s stand for weak covalent bonds and strong covalent bonds, respectively.

Table SA1. Proposed definitions for the classification and characterization of interactions by the signs $H_b(\boldsymbol{r}_c)$ and $H_b(\boldsymbol{r}_c) - V_b(\boldsymbol{r}_c)/2$ and their first derivatives, together with the tentatively proposed definitions by the characteristic points on the plots of $H_b(\boldsymbol{r}_c)$ versus $H_b(\boldsymbol{r}_c) - V_b(\boldsymbol{r}_c)/2$. The tentatively proposed definitions are shown by italic. The requirements for the interactions are also shown.

ChP/Interaction	Requirements by $H_b(\boldsymbol{r}_c)$ and $V_b(\boldsymbol{r}_c)$	Requirements by $G_b(\boldsymbol{r}_c)$ and $V_b(\boldsymbol{r}_c)$
Origin	$H_b(\boldsymbol{r}_c) - V_b(\boldsymbol{r}_c)/2 = 0$; $H_b(\boldsymbol{r}_c) = 0$	$G_b(\boldsymbol{r}_c) = 0$; $V_b(\boldsymbol{r}_c) = 0$
vdW	$H_b(\boldsymbol{r}_c) > 0$; $dH_b(\boldsymbol{r}_c)/d(-r) > 0$	$G_b(\boldsymbol{r}_c) > -V_b(\boldsymbol{r}_c)$; $dG_b(\boldsymbol{r}_c)/d(-r) > -dV_b(\boldsymbol{r}_c)/d(-r)$
Borderline (BD-1)	$H_b(\boldsymbol{r}_c) > 0$; $dH_b(\boldsymbol{r}_c)/d(-r) = 0$	$G_b(\boldsymbol{r}_c) > -V_b(\boldsymbol{r}_c)$; $dG_b(\boldsymbol{r}_c)/d(-r) = -dV_b(\boldsymbol{r}_c)/d(-r)$
t-HB$_{\text{with no covalency}}$	$H_b(\boldsymbol{r}_c) > 0$; $dH_b(\boldsymbol{r}_c)/d(-r) < 0$	$G_b(\boldsymbol{r}_c) > -V_b(\boldsymbol{r}_c)$; $dG_b(\boldsymbol{r}_c) < -dV_b(\boldsymbol{r}_c)$
Borderline (x-intercept)	$H_b(\boldsymbol{r}_c) = 0$ ($\theta_p{}^a = 125^o$)	$G_b(\boldsymbol{r}_c) = -V_b(\boldsymbol{r}_c)$ ($\theta_p{}^a = 125^o$)
t-HB$_{\text{with covalency}}$	$H_b(\boldsymbol{r}_c) < 0$; ($125^o <$) $\theta_p{}^a < 150^o$	$G_b(\boldsymbol{r}_c) < -V_b(\boldsymbol{r}_c)$; ($125^o <$) $\theta_p{}^b < 150^o$
Borderline (Tentative)	*$\theta_p{}^a = 150^o$*	*$\theta_p{}^b = 150^o$*
CT-MC	$d(H_b(\boldsymbol{r}_c) - V_b(\boldsymbol{r}_c)/2)/d(-r) > 0$;	$dG_b(\boldsymbol{r}_c) > dV_b(\boldsymbol{r}_c)/2$;
	$150^o < \theta_p{}^a < 180^o$	$150^o < \theta_p{}^a < 180^o$
Borderline (BD-2)	$d(H_b(\boldsymbol{r}_c) - V_b(\boldsymbol{r}_c)/2)/d(-r) = 0$	$2dG_b(\boldsymbol{r}_c)/d(-r) = -dV_b(\boldsymbol{r}_c)/d(-r)$
	($H_b(\boldsymbol{r}_c) - V_b(\boldsymbol{r}_c)/2 > 0$; $H_b(\boldsymbol{r}_c) < 0$)	($-V_b(\boldsymbol{r}_c)/2 < G_b(\boldsymbol{r}_c) < -V_b(\boldsymbol{r}_c)$)
CT-TBP with X_3^-	$d(H_b(\boldsymbol{r}_c) - V_b(\boldsymbol{r}_c)/2)/d(-r) < 0$	$2dG_b(\boldsymbol{r}_c)/d(-r) < -dV_b(\boldsymbol{r}_c)/d(-r)$
	($H_b(\boldsymbol{r}_c) - V_b(\boldsymbol{r}_c)/2 > 0$; $H_b(\boldsymbol{r}_c) < 0$)	($-V_b(\boldsymbol{r}_c)/2 < G_b(\boldsymbol{r}_c) < -V_b(\boldsymbol{r}_c)$)
Borderline (y-intercept)	$H_b(\boldsymbol{r}_c) - V_b(\boldsymbol{r}_c)/2 = 0$ ($H_b(\boldsymbol{r}_c) < 0$)	$G_b(\boldsymbol{r}_c) = -V_b(\boldsymbol{r}_c)/2$ ($G_b(\boldsymbol{r}_c) < -V_b(\boldsymbol{r}_c)$)
Cov-w	$H_b(\boldsymbol{r}_c) - V_b(\boldsymbol{r}_c)/2 < 0$; *$R^c < 0.15$ au*	$G_b(\boldsymbol{r}_c) < -V_b(\boldsymbol{r}_c)/2$; *$R^c < 0.15$ au*
Borderline (Tentative)	*$R^c = 0.15$ au*	*$R^d = 0.15$ au*
Cov-s	$H_b(\boldsymbol{r}_c) - V_b(\boldsymbol{r}_c)/2 < 0$; *$R^c > 0.15$ au*	$G_b(\boldsymbol{r}_c) < -V_b(\boldsymbol{r}_c)/2$; *$R^d > 0.15$ au*

[a] $\theta_p = 90^o - \tan^{-1}[dH_b(\boldsymbol{r}_c)/d(H_b(\boldsymbol{r}_c) - V_b(\boldsymbol{r}_c)/2)]$, $\theta_p = 125^o$ is tentatively given for $\theta = 90^o$, where θ is defined by $90^o - \tan^{-1}[H_b(\boldsymbol{r}_c)/(H_b(\boldsymbol{r}_c) - V_b(\boldsymbol{r}_c)/2)]$ with $H_b(\boldsymbol{r}_c) = 0$. [b] $\theta_p = 90^o - \tan^{-1}[d(G_b(\boldsymbol{r}_c) + V_b(\boldsymbol{r}_c))/d(G_b(\boldsymbol{r}_c) + V_b(\boldsymbol{r}_c)/2)]$, $\theta_p = 125^o$ is tentatively given for $\theta = 90^o$, where θ is defined by $90^o - \tan^{-1}[(G_b(\boldsymbol{r}_c) + V_b(\boldsymbol{r}_c))/(G_b(\boldsymbol{r}_c) + V_b(\boldsymbol{r}_c)/2)]$ with $(G_b(\boldsymbol{r}_c) + V_b(\boldsymbol{r}_c)) = 0]$. [c] $R = [(H_b(\boldsymbol{r}_c) - V_b(\boldsymbol{r}_c)/2)^2 + (H_b(\boldsymbol{r}_c))^2]^{1/2}$. [d] $R = [(G_b(\boldsymbol{r}_c) + V_b(\boldsymbol{r}_c)/2)^2 + (G_b(\boldsymbol{r}_c) + V_b(\boldsymbol{r}_c))^2]^{1/2}$.

References

SA1 (a) *Atoms in Molecules. A Quantum Theory*, ed. R. F. W. Bader, Oxford University Press, Oxford, UK, 1990; (b) C. F. Matta and R. J. Boyd, *An Introduction to the Quantum Theory of Atoms in Molecules In The Quantum Theory of Atoms in Molecules: From Solid State to DNA and Drug Design*, eds. C. F. Matta and R. J. Boyd, WILEY-VCH, Weinheim, Germany, 2007, ch. 1.

SA2 (a) R. F. W. Bader, T. S. Slee. D. Cremer and E. Kraka, *J. Am. Chem. Soc.* 1983, **105**, 5061–5068; (b) R. F. W. Bader, *Chem. Rev.* 1991, **91**, 893–926; (c) R. F. W. Bader, *J. Phys. Chem. A* 1998, **102**, 7314–7323; (d) F. Biegler-König, R. F. W. Bader and T. H. Tang, *J. Comput. Chem.* 1982, **3**, 317–328; (e) R. F. W. Bader, *Acc. Chem. Res.* 1985, **18**, 9–15; (f) T. H. Tang, R. F. W. Bader and P. MacDougall, *Inorg. Chem.* 1985, **24**, 2047–2053; (g) F. Biegler-König, J. Schönbohm and D. Bayles, *J. Comput. Chem*. 2001, **22**, 545–559; (h) F. Biegler-König and J. Schönbohm, *J. Comput. Chem.* 2002, **23**, 1489–1494.

SA3 W. Nakanishi, T. Nakamoto, S. Hayashi, T. Sasamori and N. Tokitoh, *Chem. Eur. J.* 2007, **13**, 255–268.

SA4 (a) W. Nakanishi, S. Hayashi and K. Narahara, *J. Phys. Chem. A* 2009, **113**, 10050–10057; (*b*) W. Nakanishi, S. Hayashi and K. Narahara, *J. Phys. Chem. A* 2008, **112**, 13593–13599.

SA5 W. Nakanishi and S. Hayashi, *Curr. Org. Chem.* 2010, **14**, 181–197.

SA6 (a) W. Nakanishi and S. Hayashi, *J. Phys. Chem. A* 2010, **114**, 7423–7430; (b) W. Nakanishi, S. Hayashi, K. Matsuiwa and M. Kitamoto, *Bull. Chem. Soc. Jpn.* 2012, **85**, 1293–1305.

SA7 W. Grimme, J. Wortmann, D. Frowein, J. Lex, G. Chen and R. Gleiter, *J. Chem. Soc., Perkin Trans. 2* 1998**,** 1893–1900.

SA8 C.-T. Lin, N.-J. Wang, Y.-L. Yeh and T.-C. Chou, Tetrahedron, 1995, **51**, 2907–2928.

SA9 E. Espinosa, I. Alkorta, J. Elguero and E. Molins, *J. Chem. Phys.* 2002, **117**, 5529. See also R. Bianchi, G. Gervasio and D. Marabello, *C. R. Chim.*, 2005, **8**, 1392.